GENE-771-59-0994 Rev.4
DRF B13-01732
JUNE, 1995

DESIGN REPORT FOR THE INSTALLATION OF STABILIZERS ON THE PEACH BOTTOM 2, 3 CORE SHROUD

GE NUCLEAR ENERGY

Prepared by: Mark O. Lenz
M.O. Lenz
Project Engineer

Verified by: N.A. McClean
N.A. McClean
Principal Engineer

Approved by: for
L.E. Tschantre
Project Manager

IMPORTANT NOTICE REGARDING

CONTENTS OF THIS REPORT

Please Read Carefully

The only undertakings of GE Nuclear Energy (GENE) respecting information in this document are contained Contract No. PB263848 between PECO Energy and GENE, as identified in the purchase order for this report (PECO Purchase Order No. PB263848) and nothing contained in this document shall be construed as changing the contract. The use of this information other than as provided therein of for any purpose other than for which it is intended, is not authorized; and with respect to any unauthorized use, GENE makes no representation or warranty, and assumes no liability as to the completeness, accuracy or usefulness of the information contained in this document, or that its use may not infringe upon privately owned rights.

Changes made to the previous revision of this report are indicated by "bars" drawn in the left margin.

Table of Contents

1.0 DESCRIPTION OF CHANGE

An in-vessel visual inspection (IVVI) of the horizontal welds in the shroud will be performed at Peach Bottom Unit 2. Based on the results of the weld inspection, shroud stabilizer assemblies, which function to replace cracked horizontal welds in the shroud, may be installed in Peach Bottom Unit 2 during the next refueling outage. In the event that the installation of the stabilizer assemblies is not required for Unit 2, the assemblies will be retained as a contingency for possible later installation, or for installation at Peach Bottom Unit 3. If the stabilizers are installed at Unit 3, replacement of the core spray line repair brackets should be considered, as discussed in Section 1.6.2.

1.1 General

Welds H1 through H7 of the core shroud will be structurally replaced by a set of 4 stabilizer assemblies. Figure 1 shows a stabilizer assembly. Each stabilizer assembly attaches to the top of the shroud and to the shroud support plate.

Radially acting stabilizer springs are used to maintain the alignment of the core shroud to the reactor pressure vessel (RPV) during seismic events. The set of stabilizers replace the structural functions of the shroud welds which are postulated to contain cracks. Each stabilizer assembly consists of a tie rod, an upper spring, a lower spring, an upper bracket, a midspan tie rod support, a lower anchor assembly, and other minor parts. The tie rod provides the vertical load carrying ability from the upper bracket to the RPV shroud support plate attachment, as well as support for the springs. The vertical locations of the radial springs were chosen to provide the maximum support for the shroud and fuel assemblies. The upper spring provides radial load carrying ability from the shroud, at the top guide elevation, to the RPV. The lower spring provides radial load carrying ability from the shroud, at the core support plate elevation, to the RPV. The upper bracket provides an attachment feature to the top of the shroud as well as restraint of the upper shroud welds. The midspan tie rod support functions to increase the natural frequencies of the stabilizer assembly.

There are seven horizontal welds (Figure 2) in the Peach Bottom 2, 3 shroud. These welds are identified as H1 through H7, with H1 being the uppermost weld and H7 being the attachment of the shroud to the shroud support cylinder. Each cylindrical section of the shroud is prevented from unacceptable motion by the stabilizers. The motion of the sections above H1, between H1 and H2, and between H2 and H3 are restrained by the upper bracket. The upper bracket contacts the shroud and is radially supported by the upper spring which contacts the RPV. There is a stop

on the upper bracket which prevents unacceptable motion of the shroud section between the H3 and H4 welds. The lower spring contacts the shroud such that it prevents unacceptable motion of the section between the H4 and H5 welds, as well as the section between the H5 and H6 welds. There is also a feature on the lower spring which prevent unacceptable motion of the shroud section between the H6 and H7 welds.

The H8 weld (Figure 2) connects the shroud support shelf to the shroud support cylinder. The assumption of cracking in the H8 weld was also considered in the seismic analysis, the analysis of the stresses in the shroud support plate, and in the systems performance evaluation with the assumption of leakage through the weld cracks.

The primary forces applied to the stabilizers are from seismic events, LOCA differential pressure loads, and differential thermal expansion. The installation of the stabilizer assemblies and the assumption of cracks in the shroud change the seismic response of the reactor internals. Thus, it was necessary to modify the seismic analysis of the reactor to include the assumed cracks and the stabilizers. This dynamic analysis was performed in a iterative manner to determine the appropriate values of the spring constants for the upper and lower springs, as well as the number of stabilizer assemblies required. It was determined that four stabilizer assemblies would be acceptable. Each assembly has an upper spring with a spring rate constant of 20,000 pounds per inch, and a lower spring with a spring rate constant of 150,000 pounds per inch. The midspan tie rod support increases the natural frequency of the rod to prevent unacceptable vibration.

1.2 Design

Significant cracking adjacent to the horizontal shroud welds has been observed at several BWRs. If significant cracking is discovered in the horizontal shroud welds at Peach Bottom Unit 2, or at Unit 3, a repair will be implemented. The repair will structurally replace all of the horizontal girth welds in the shroud with a set of shroud stabilizers.

The core shroud is a safety related component. It provides horizontal support for the fuel assemblies, control rods, and incore instrumentation. It provides vertical support for the peripheral fuel assemblies, top guide, and core support plate. It also provides a floodable volume inside the reactor pressure vessel (RPV), which is necessary in the event of a Loss of Coolant Accident (LOCA). Note, however, that welds H1 through H3 are above the floodable volume. In addition, the shroud supports the core spray spargers and the core spray lines.

The stabilizers were designed to the structural criteria specified in the original Peach Bottom 2, 3 UFSAR. The ASME Code, Section III, Subsection NG was used as an analysis guide. The

stabilizers were designed to the requirements of References 4.1 and 4.2. Reference 4.1 is the design specification for the stabilizers, exclusive of ASME Code aspects. Reference 4.2 contains the ASME Code requirements for the interfaces of the stabilizers with the RPV, since the installation of the stabilizers will result in new loads being applied to the RPV. All of the loads and load combinations specified in the UFSAR, that are relevant to the core shroud, are included in the design specifications. The increased operating pressures due to Power Rerate and increased core flow are also included in the design specifications.

The stabilizers are installed with a small vertical mechanical preload, which assures that all components are tight and which provides approximately 3300 pounds of axial load on the 3.5 inch diameter tie rods. The upper support, upper spring, lower spring, and lower anchor assembly are fabricated from alloy X-750, which has a smaller coefficient of thermal expansion than does the 304 stainless steel shroud. Additionally, the tie rods are fabricated from XM-19 stainless steel, which also has a smaller coefficient of thermal expansion than does the shroud. Thus the stabilizer assemblies are thermally preloaded when the reactor is at operating conditions. The spring constant of the stabilizers in the vertical direction was designed to yield a total vertical preload at operating conditions of greater than the net upward applied loads on the shroud. The vertical loads are largely a result of the differential pressures across the shroud head and across the core support plate. Thus, if any or all of the H1 through H7 welds were completely cracked, the stabilizers will vertically restrain the shroud such that no vertical displacement will occur during Normal operation, which minimizes potential leakage through the assumed cracks.

The upper and lower springs are installed with a small radial preload such that they provide radial support for the shroud. During Normal operation, the shroud and springs radially expand due to thermal growth slightly more than the RPV due to both thermal and pressure, which increases the radial preload and assures that the springs provide linear support for the shroud during normal operation.

The vertical location of the upper and lower springs were chosen to provide the maximum horizontal support for the fuel assemblies. The upper springs are at the top guide elevation and the lower springs are at the core support plate elevation. All of the horizontal support for the fuel assemblies is provided by the top guide and the core support plate.

The stabilizer assemblies are designed and fabricated as safety related components, as is the requirement for the shroud. The installation of the stabilizer assemblies will replace the functions of welds H1 through H7.

At the top, each stabilizer assembly fits through two slots, which are machined through the non-safety related shroud head and steam separator assembly. The stabilizer upper bracket contacts the top surface and the inside surface of the shroud flange. It then extends downward to below weld H3. It supports the upper spring, and has a hole through which the tie rod passes. The tie rod is held against the upper bracket with a nut. The tie rod extends downward approximately 165 inches to the lower spring. At the middle of the tie rod there is a support between the tie rod and the RPV. The support is installed such that there is a horizontal preload between the tie rod and the RPV. The midspan support functions to minimize the potential for vibration of the stabilizer assembly. At the bottom, the tie rod threads into the lower spring. The lower spring has a clevis at the bottom, which is attached to the pin in the lower support. The lower support is bolted to the shroud support plate with two toggle bolts.

All pieces of the stabilizer assemblies are locked in place with mechanical devices. Loose pieces can not occur without the failure of a locking device. The stresses in the stabilizer components during Normal plant operation are less than the Normal event allowable stresses. The stabilizers are fabricated from stress corrosion resistant material. Therefore, it is very unlikely that a stabilizer component will fail.

The fast flux levels at the stabilizers are low compared with the values which could result in the degradation of material properties. After 20 years of operation, the maximum fast fluence at the stabilizers will be approximately 3.0E19 n/cm^2, which is well below the value to cause damage to stainless steel.

1.3 Materials

The stabilizers are fabricated entirely from the type 316 stainless steel, XM-19 stainless steel, and alloy X-750. There is no welding required.

The upper and lower springs, upper nut, upper bracket, and lower support are fabricated from Alloy X-750 (Ni-Cr-Fe) material that has been heat treated at 1975 ± 25°F followed by an air cool and then age hardened to increase its strength. The annealing and age hardening processes used are essentially the same as those used on the improved jet pump beams for maximum resistance to IGSCC initiation. As a control for intergranular attack (IGA), a minimum of 0.030 inches of material is removed after the last high temperature annealing operation. This material is certified to ASTM B637, Grade UNS N07750. Alloy X-750 was chosen because high strength was required, and it has a coefficient of thermal expansion that is less than that of the shroud.

Alloy X-750 is resistant to IGSCC at the stress levels the components will experience during operation, which is less sustained tensile stress than the jet pump beams experience. Some smaller components are also fabricated from alloy X-750. The cobalt content of all X-750 material was limited to a maximum of 0.09 %.

The tie rods are fabricated from XM-19 stainless steel with a maximum carbon content of 0.04%. The XM-19 rods were solution annealed at 2000 $\pm$ 50^{0}F, and tested for evidence of sensitization and IGA. XM-19 stainless steel was chosen for the fabrication of the tie rods because of its higher strength over that of 300 series stainless steel.

Other components are fabricated from type 316 stainless steel material with a maximum carbon content of 0.02%. The material was annealed at 1900 to 2100 degrees F followed by quenching in circulating water to a temperature below 400 degrees F. All material was tested for evidence of sensitization and IGA.

1.4 System Performance Evaluation

The installation of the four shroud stabilizer assemblies at Peach Bottom Unit 2 or 3 requires the machining of four pairs of holes through the shroud head flange. Each of these holes will have some clearance after the installation of the upper support, which will allow a small amount of leakage flow to bypass the steam separation system. In addition, four pairs of holes will be machined in the shroud support plate, which will also allow a small amount of core flow leakage through the clearance between the holes and the mating bolts. There are seven horizontal welds in the shroud, with two welds below the core plate, and five welds above the core plate. These welds may develop cracks, which will present additional small leakage flow paths for the core flow. In addition, potential leakage through cracks in the H8 weld has been considered. Finally, leakage past the replacement access hole covers in the shroud support shelf has been predicted to be 0.07% of core flow. This section summarizes the performance impact of the total leakage flow for up to 110% of rated power, and 87% to 110% of rated core flow (i.e., potential future power rerate conditions).

Leakage flow past the replacement access hole covers is 0.07% of core flow. Leakage from the machined holes in the shroud head flange is assumed to be two-phase fluid at the core exit quality. The maximum leakage through these eight holes is predicted to be equal to 0.10% of core flow. The steam portion of this leakage will contribute to increasing the total carryunder from the steam separators. The cumulative leakage flow from the shroud support plate holes and

from the assumed weld cracks is conservatively estimated to be 0.21% of core flow. The impact of the total leakage on the performance of the steam separation system, the performance of the jet pumps, the fuel thermal margin, emergency core cooling system (ECCS) performance, and the length of the fuel cycle have been evaluated as summarized in the following subsections.

1.4.1 Steam Separation System

The shroud leakage flow includes steam flow, which effectively increases the total carryunder in the downcomer by a maximum of about 0.02% at 110% rated power, and 87% to 110% rated core flow. The total leakage flow also has the effect of slightly decreasing the flow per separator, and slightly increasing the separator inlet quality. The carryunder from the separators is based on the applicable separator test data at the lower limit of the operating water level range. The combined effective carryunder from the separators and from the shroud leakage at 87% and 110% rated core flow is about 0.28% and 0.25% respectively. The specified design value corresponding to 0.25% is slightly exceeded, but is acceptable. The impact of the increased carryunder is evaluated in the following subsections. The carryover from the separators remains within the design limits, so that moisture from the steam dryer meets the plant performance requirement of less than 0.1%.

1.4.2 Jet Pumps

The increased total carryunder will decrease the subcooling of the flow in the downcomer. This in turn reduces the operating margin to jet pump cavitation. Any increase in flow resistance in the annulus due to the installation of the shroud stabilizer assemblies will be insignificant. The results show that, although that the jet pump cavitation operating margin decreases slightly, it will remain adequate. The change in cavitation operating margin is not significant enough to require a change to a cavitation set point, or to the power flow map.

1.4.3 Anticipated Operational Transients

The computer code used to evaluate performance under plant transients and to calculate fuel thermal margin includes carryunder as one of the inputs. There will be a slight increase in carryunder due to shroud head installation hole leakage. The increase in carryunder results in an insignificant decrease in subcooling in the downcomer region, with a corresponding decrease in core inlet subcooling. The leakage flow rate via the shroud support plate holes and the shroud weld cracks tends to (insignificantly) reduce the coolant flow rate into the core region. This core flow reduction will slightly decrease the core inlet subcooling. However, the total core flow reduction, and the core inlet subcooling changes are both within the sensitivity range of the

critical power ratio (CPR) calculations. Also, the increased carryunder fraction will tend to reduce (make milder) the response from pressurization transients. Therefore, the fuel thermal limits will not be affected.

1.4.4 Emergency Core Cooling System

The effect of the shroud and access hole cover leakage flows is to decrease the time to core uncovery slightly, and also to increase the time that the core is uncovered. An evaluation of the ECCS performance, conservatively based on the cumulative effect of leakage at the shroud head, at the shroud support plate holes, for five full (360^0) shroud weld cracks, and at the access hole covers, was performed. The combined effects have been determined to increase the peak cladding temperature (PCT) for the limiting LOCA event by less than 20^0F. This increase is sufficiently small to be judged insignificant, and thus, the licensing basis PCT for the Normal operation condition with no shroud leakage is applicable. In addition, the licensing basis PCT was calculated assuming a 20% reduction in the ECCS flow rates. The effect of the ECCS flow rate reduction bounds the effects of the assumed shroud leakage. The sequence of events remains essentially unchanged for the LOCA events with the shroud leakage.

The conservative ECCS flow rates in the current LOCA analysis significantly bound all potential flow losses resulting from the installation of the shroud stabilizers, and thus the current ECCS-LOCA analysis remains valid. However, even if the current ECCS-LOCA analysis did not use reduced ECCS flow rates, the calculated PCT (1690^0F + 20^0F) would remain well below the regulatory PCT limit (2200^0F), the change in PCT would be less than the 50^0F requirement for NRC notification, and a floodable volume to 2/3 core height will be maintained.

1.4.5 Fuel Cycle Length

The cumulative leakage flow results in an increase in the core inlet enthalpy by about 0.1 Btu/lb, compared with the no leakage condition. The combined impact of the reduced core inlet subcooling and the reduced core flow due to the leakage results in a minor effect (approximately 0.8 days) on fuel cycle length, and is considered negligible.

1.4.6 Leakage through Shroud Cracks and Shroud Support Plate Holes

The amount of leakage that would pass through an assumed 360° through wall crack at operating conditions is limited by the tie rods, which hold the crack surfaces in contact. If it is conservatively estimated that the crack can be modeled as a 0.001 inch wide smooth slit through the shroud, then the leakage is approximately 145 GPM for all seven welds combined. If the H8

weld is assumed to be cracked, the combined leakage for all eight welds is approximately 170 GPM. All of the leakage below the core plate would be water of the same temperature as the water in the downcomer. All of the leakage between the top guide and the core plate would be water. Only the leakage from H1 and H2 would include any steam. The leakage through the eight machined mounting holes in the shroud support plate will not be more than 525 GPM, calculated at rated power and Increased Core Flow.

Summary of Leakage Flows at Uprated Power and ICF

Pressure difference (psi)	
Shroud Head	9.41
Upper Shroud	9.35
Lower Shroud	33.0
Leakage Flow (gpm)	
Repair Holes in Shroud Head	1105
Weld Cracks	170
Repair Holes in Support Plate	525
Access Hole Covers	215
Leakage to Core Mass Flow (%)	
Repair Holes in Shroud Head	0.10
Weld Cracks	0.04
Repair Holes in Support Plate	0.17
Access Hole Covers	0.07

1.4.7 Conclusions

The stabilizer assemblies will not significantly affect the flow within the downcomer and will not adversely affect the performance of any reactor internal. The water inventory in the downcomer with the stabilizers installed exceeds the volume used in the existing analyses.

The cumulative effects of leakage at the shroud head flange, shroud support plate holes, assumed shroud weld cracks, and access hole covers have been evaluated for degradation in steam separation system performance, jet pump performance, fuel thermal margin, ECCS system performance, and for changes in fuel cycle length. The leakage flows are sufficiently small so that steam separation system performance, jet pump performance, fuel thermal margin, and fuel

cycle length are not significantly affected. Also, the effect on ECCS performance is sufficiently small to be judged insignificant, and thus, the licensing basis PCT for Normal operation with no shroud leakage is applicable.

1.5 Seismic Analysis

A seismic analysis of Peach Bottom Unit 2, and 3 has been performed (Reference 4.8). The new seismic model incorporated the installation of the shroud stabilizers. Included in the analysis were the determination of the natural frequencies and mode shapes of the RPV building system for the E-W and N-S direction, computation of the dynamic response to the DBE and MCE time histories, and the calculation of the shears, moments, and displacements. The building model was the 1970 model specified by the architect engineers (Bechtel). The Design Earthquake (DBE) and Maximum Credible Earthquake (MCE) time histories used are based on response spectra in Figures C.3.1 and C.3.2 of the Peach Bottom 2, 3 Updated Final Safety Analysis Report (Reference 4.3). Peak ground accelerations for the DBE and MCE are 0.05g and 0.12g respectively (Reference 4.3)

The model was qualified by achieving excellent agreement with frequencies and mode shapes predicted by the previous GE model of Reference 4.5. The synthetic time history was generated from the design response spectra.

The computer program SAP4G07 (Reference 4.4) was used in this study. Transient response analysis with modal superposition method (NDYN=12) was adapted. A solution time step of 0.002 second was chosen, according to the user's manual for this linear analysis.

The vertical seismic effect was combined directly with the horizontal seismic load (either North-South or East-West). Forces and moments due to vertical loading were calculated as a multiplier of the dead weight. This is based on the approach discussed in the UFSAR (Reference 4.3).

The springs for the stabilizer supports and tie-rods are included in the model. Each stabilizer assembly has a radial spring at both the top guide and at the core support plate elevation. Each radial spring can take only compressive loads. The axial spring constant for the tie-rods was calculated based on the four tie-rods rotating about the shroud neutral axis

In order to determine that the installation of shroud stabilizers does not adversely affect the existing structural integrity with the assumption that no defective welds are present in the shroud, analyses for the uncracked case were performed with the shroud stabilizers in place. The results in this study were compared with those given in Reference 4.5 to insure that all the RPV and internals loads and displacements are within the allowable limits.

An enveloping combination of cracked/uncracked welds has been determined to define the worst situation for the core plate and top guide displacements, in order to insure control rod insertion and plant shut-down. Each cracked weld was postulated to have a 360 degree through wall crack. Seven individual cracked welds as well as several combinations of two cracked welds have been evaluated. Also, an all cracked combination has been evaluated. Each 360 degree through wall crack has been modeled as a hinge or a roller to determine the limiting boundary conditions. The specific load combination that is being analyzed also influences the choice of the boundary condition of hinge or roller. For example, during Normal operation differential thermal tightening of the tie rods prevents upward motion of the shroud. Thus, the tie rods hold the crack surfaces in contact, which assures that a hinge boundary condition is conservative. During a main steam line LOCA, the tie rods will momentarily stretch such that the crack surfaces in the shroud may part. This condition can only exist for a few seconds while the shroud head pressure drop is sufficient to stretch the tie rods. During this short period of time, the assumption of a roller is appropriate. The seismic analysis conservatively assumes that the roller assumption applies during the entire seismic time history.

For the LOCA case with all welds cracked, the uppermost weld (H1) is postulated to be a roller and all the other cracks are postulated as hinges. In this case, to prevent modeling instability, additional torsional and translational springs with small spring rates were inserted at the cracks to stabilize the mathematical model for the all cracked case. In reality, these small torsional springs represent certain degree of resistance from the structure. It was found, through a sensitivity study, that the analysis results were not affected by the small spring rates that were chosen.

The seismic time history analysis considered a total of 21 load cases. They represent combinations of two earthquake events (DBE and MCE), two horizontal directions (North-South and East-West), several cracked weld assumptions, and the two Peach Bottom units.

The maximum deflection of any part of the shroud that is not directly supported by either the upper or lower radial springs is limited to approximately 1.0 inch by mechanical limit stops. These stops do not perform any function unless a section of the shroud, for example the section between the H4 and H5 welds, becomes loose and a combined LOCA plus seismic event occurs.

If this unlikely scenario were to occur, the stops will limit the horizontal displacement of the shroud section to approximately 1.0 inch, which is equal to one half of the shroud wall thickness. These stops do not invalidate the linear seismic analysis. A displacement equal to one half of the shroud wall thickness will not result in post event leakages that prevent core cooling, because the shroud sections still overlap each other by one half (1.0 inch) of the shroud wall thickness.

The original seismic model of the NSSS was revised to incorporate the current core reload and the installation of the shroud stabilizers. This case models the current configuration with an uncracked shroud. The seismic response of this model was then determined using a ground motion input time history equivalent to the Design Response Spectra. A comparison of the results with those from the original seismic analysis showed a close comparison with all resulting loads in NSSS components, which were well below the allowable values. The updated model was then modified to reflect postulated 360 degree through wall cracking at the H1 through H7 shroud welds. Various combinations of postulated cracking locations were investigated in order to identify the bounding combinations and locations. The shroud stabilizers are intended to relieve the shroud seismic overturning moment, and transfer it to the stabilizers and to the RPV. The modeling and the resulting seismic loads in the shroud reflect this design concept, the bending moments in the cracked and stabilized shroud being only 2% of those from the original seismic analysis reported in the UFSAR.

Potential cracking in the H8 weld between the shroud support plate and the shroud support cylinder was also evaluated. Assumed cracking at the H8 weld was determined to have no significant effect on the properties of the seismic model, and thus had no significant effect on the results of the seismic analysis.

1.6 Design Evaluation

The results of the structural evaluations per References 4.1 and 4.2 are documented in References 4.6 and 4.7. Reference 4.6 addresses the ASME Code, Section III, RPV and Reference 4.7 addresses the non-code shroud stabilizers, shroud, and shroud support shelf. The stabilizers and affected shroud and RPV components are shown to satisfy the UFSAR structural requirements using the UFSAR load combinations.

The displacements of the core support plate and the top guide are limited to the allowable displacements given in Reference, 4.1 for all load combinations.

1.6.1 Load Combinations

The UFSAR requires evaluation of Normal operating loads as well as DBE, MCE, main steam line LOCA, and recirculation line LOCA. The following load combination and their classification were considered:

Normal:	Normal operating pressure differences, temperatures, and weight
Upset 1:	Normal operating weight, temperature and pressures, plus DBE
Upset 2:	Limiting thermal condition, plus Normal pressure differences and weight
Emergency 1:	Normal operating weight, temperature and pressures plus MCE
Emergency 2:	Weight plus main steam line LOCA pressure differences
Faulted 1:	Weight, plus MCE, plus main steam line LOCA pressure differences
Faulted 2:	Weight, plus MCE, plus recirculation line LOCA pressure differences

The values of the individual loads on the shroud stabilizer springs and tie-rod were obtained from the design specifications (References 4.1 and 4.2), which included the seismic analysis of the degraded shroud with stabilizers. The seismic loads in the design specifications are the limiting values of the various assumed cracking conditions.

In general, the limiting loads in the tie rods occur with different assumed shroud cracks than for the limiting radial loads in the upper and lower springs. It was conservatively assumed that the worst loads on each component in each direction would be combined. The limiting loads in the tie rods occur when it is assumed that there is a 360 degree through wall crack in weld H7 and that crack behaves as a hinge (shear transfer but no moment transfer). If the H7 is assumed to behave as a roller (no shear and no moment transfer), then the loads are reduced in the tie rods. The limiting loads in the radial direction on the upper springs occur when it is assumed that all of the horizontal girth welds in the shroud have 360 degree through wall cracks, with each of these joints modeled as hinges. The limiting radial loads on the lower spring occur with only the H7 cracked, and the joint modeled as a roller. Since the crack surfaces are held in intimate contact, the jagged IGSCC cracks can transmit shear, which is the hinge condition. During a main steam

line break the upward pressure forces are sufficient, for a short period of time, to stretch the tie rods and allow the crack surfaces to separate. For this situation, the roller case was assumed at the joints.

1.6.2 Results

The potential for flow induced vibration has been evaluated by calculating the lowest natural frequency of the shroud stabilizer assemblies, and conservatively calculating the highest vortex shedding frequency due to the water flow across the stabilizer tie rods, in the downcomer (RPV-shroud annulus). The lowest natural frequency of the assembly is 45.5 Hertz and the maximum vortex shedding frequency is 5.2 Hertz.

There will be essentially no fatigue usage for any of the stabilizer components.

References 4.6 and 4.7 document that all structural limits have been satisfied for the shroud, shroud support plate, shroud stabilizers, and the reactor pressure vessel. The analysis of the shroud support plate considered cracking at the H8 weld. The predicted worst case transient deflections of the core plate is 0.87 inch for a load combination of a MCE with the H7 weld cracked plus a main steam pipe LOCA. The allowable transient displacement for this Faulted event is 1.49 inch. All calculated stress intensities in the lower radial spring meet the UFSAR allowables. The predicted worst case transient displacement of the top guide is 2.20 inches for a MCE with an all cracked shroud. The allowable permanent deflection of the top guide for this Emergency event is 1.40 inch. The 2.20 inch displacement is a momentary value which occurs during the MCE, and is not permanent. The stresses in the upper radial spring meet the UFSAR allowables for an Emergency event with sufficient margin such that the spring remains elastic, and the permanent displacement is zero. The predicted deflections of both the top guide and the core plate for all load combinations are within the allowables defined in the design specification, which are based on test results and the criteria of the UFSAR.

The Peach Bottom 2, 3 core spray lines were analyzed for the increase in seismic loads and anchor movements which may result from the assumption of a worst case cracked shroud, with the installation of the shroud stabilizers. The non-ASME Code, Safety Related, core spray lines were conservatively analyzed using the rules for Class I piping in the ASME Code Section III, NB-3600, as an analysis guide. It was determined that the Peach Bottom core spray lines as originally designed meet the ASME Code allowables for stress and fatigue usage for Normal / Upset, Emergency, and Faulted conditions, and thus remain functional with the assumption of a

cracked shroud, and the installation of the shroud stabilizers. The allowable stress limits are in accordance with Tables C.5.2 and C.5.5 of the Peach Bottom UFSAR.

Each core spray line attaches to the reactor pressure vessel at the 120^0 or the 240^0 core spray nozzle. Each line branches into a 6.0" schd. 40 horizontal header, with two vertical downcomers that are welded to elbows in the upper shroud. The increase in loads on the core spray lines are largely a result of the increase in movement of the assumed worst case cracked shroud during a seismic event, or loss of cooling accident (LOCA). The shroud displacements are documented in Reference 4.8. The core spray lines with the mounting brackets, and appropriate boundary conditions were modeled with the ANSYS Revision 4 finite element computer program.

The load combinations addressed were as follows:

Service Level	Load Combination	Stress Type
N /U	Weight + $DE_{Inertia}$	Primary
N/U	Thermal + $DE_{Inertia}$ + $DE_{Anchor\ Movement}$	Primary + Secondary
E	Weight + $MCE_{Inertia}$	Primary
F	Weight + $MCE_{Inertia}$	Primary

All calculated stresses in the core spray piping met the ASME Code stress allowables. The maximum 40 year fatigue usage was calculated to be less than the Code allowable of 1.0. The Normal / Upset condition for primary plus secondary stress included the existing thermal stresses due to thermal expansion and thermal anchor movements, as well as seismic inertia and seismic anchor movements.

It should be noted that , per NB-3217-2, the stresses resulting from piping anchor point motions are considered to be secondary, and are not required to be evaluated for Emergency and Faulted conditions (one time load application), in accordance with the requirements of NB-3600. However, as a functional check on the core spray lines during the anchor movement resulting from a Faulted Condition main steam line LOCA combined with a maximum credible earthquake (MCE) event, the maximum strain in the piping was calculated. This was found to be less than 1.0%, which is well below the minimum allowable strain at failure of 25% for ASTM A-312

conditions (one time load application), in accordance with the requirements of NB-3600. However, as a functional check on the core spray lines during the anchor movement resulting from a Faulted Condition main steam line LOCA combined with a maximum credible earthquake (MCE) event, the maximum strain in the piping was calculated. This was found to be less than 1.0%, which is well below the minimum allowable strain at failure of 25% for ASTM A-312 TP304 stainless steel piping, thus demonstrating the functionality of the core spray line after a Faulted event. The displacement of the shroud during a recirculation line LOCA was not found to be significant.

Repair brackets were installed on the core spray lines at Peach Bottom Unit 3 in 1985 (Reference 4.12) after the discovery of cracking in the 240^{0} core spray line header near the connection of the pipe with the tee-box. The brackets are welded to the tee-box and to each header pipe, with one bracket mounted above the tee-box, and one mounted below. The core spray lines and repair brackets were also modeled and analyzed with the assumption of a 360 degree crack in each header pipe. The core spray piping was determined to meet the allowables for stress and fatigue usage in accordance with the requirements of NB-3600. The repair brackets and attachment welds to the piping were analyzed in accordance with the requirements of NB-3200. The stresses in the repair brackets and attachment welds were determined to meet ASME Code primary stress allowables for all load cases.

Although the ASME Code Primary and Primary plus Secondary stress criteria is satisfied, the fatigue usage in a local area of the bracket to pipe weld for one of the two repair brackets was calculated to be 2.0, which is in excess of the Code allowable of 1.0. The fatigue usage for the second repair bracket was found to be acceptable. The main contribution to the calculated fatigue usage was due to the relative displacement of the shroud during 10 full amplitude cycles of a design earthquake (DE) event. A stress concentration factor of 4.0 was assumed for the fillet welds between the repair brackets and the core spray piping.

The analysis of the core spray line header tee-box repair brackets described above does not support the plant design basis of 50 DE earthquake cycles, as indicated in Section C.5.3.6 of the Peach Bottom UFSAR, with the core shroud horizontal welds postulated to be fully cracked and the core shroud stabilizers installed (Modification P00435). Therefore, PECO Modification P00541 has been initiated to provide a revised analysis which demonstrates that the repair brackets are acceptable with Modification P00435 installed, or to provide replacement brackets that meet the design requirements. Modification P00541 will be installed prior to, or during the implementation of the core shroud stabilizer modification.

2.0 REASON FOR CHANGE

Cracks have been observed in the core shrouds of several BWRs. The NRC has issued a generic letter, Reference 4.9, which required inspection or repair. This report discusses the installation of shroud stabilizers that will functionally replace horizontal welds H1 through H7 in the Peach Bottom 2 and 3 shroud. At this time it is not known if there are any actual cracks in the shroud. This report is based on the assumption that all of the horizontal girth welds (H1-H7) have significant cracking. However, there is no degradation of function if the stabilizers are installed in the absence of cracks in the shroud welds.

3.0 DESIGN AND LICENSING DOCUMENTATION REVIEW

The Peach Bottom 2, and 3 UFSAR (Reference 4.3) was reviewed. The results of that review are as follows. The numbers in ( ) are the paragraph numbers from which the information was extracted.

(3.3.4.1.1)	Gives a brief description of the shroud
(3.3.5.1.2)	Defines the pressure differences for Normal operation
(3.3.5.2)	Defines recirculation line LOCA pressure differences
(3.3.5.3)	Defines main steam line LOCA pressure differences
(Table 4.2.1)	Defines RPV material
(Table C.5.9)	Defines the damping values to be used in seismic analysis
(Figures C.3.1, C.3.2)	Seismic response spectra
(C.5.3.2.3)	Internals seismic analysis methodology
(Table C.5.5)	Defines the required load combinations and required safety factors
(Table C.5.1)	Defines the allowable deflections
(Table C.5.2)	Defines stress limits

(Table C.5.6)	Defines load combinations and stress limits
(C.5.3.2)	States that ASME Section III was used as a guide in the design of the reactor internals.
(Appendix K)	RPV summary stress report

4.0 REFERENCES

4.1 25A5579 Rev. 3 "Shroud Stabilizer Hardware; Design Specification".

4.2 25A5580 Rev. 4"Shroud Stabilizer; Code Design Specification".

4.3 Peach Bottom Units 2 and 3 UFSAR, Rev. 12.

4.4 SAP4G07 Computer Program.

4.5 383HA691 Rev. 0; "Seismic Analysis of Peach Bottom 2 Reactor Vessel and Internals".

4.6 25A5607 Rev. 4; "Reactor Pressure Vessel; Code Stress Report".

4.7 GENE-771-58-0994 Rev. 4; "Shroud and Shroud Stabilizer Hardware Stress Analysis".

4.8 GENE-771-60-0994 Rev 2; "Peach Bottom Seismic Analysis, Shroud Mechanical Repair Program".

4.9 NRC Generic Letter 94-03, July 25, 1994, "Intergranular Stress Corrosion Cracking of Core Shrouds in Boiling Water Reactors".

4.10 10CFR50.59 Review, Rev.0, for Mod P00435; "Installation of Stabilizers on Core Shroud In Peach Bottom Atomic Power Station Units 2 & 3".

4.11 105E1455 G001; Reactor Modification Drawing

12 797E551 G001; Core Spray Line Repair (Unit 3)

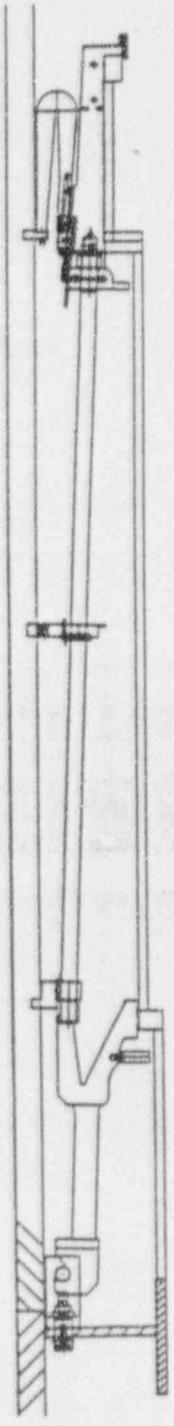

STABILIZER ASSEMBLY

FIGURE 1

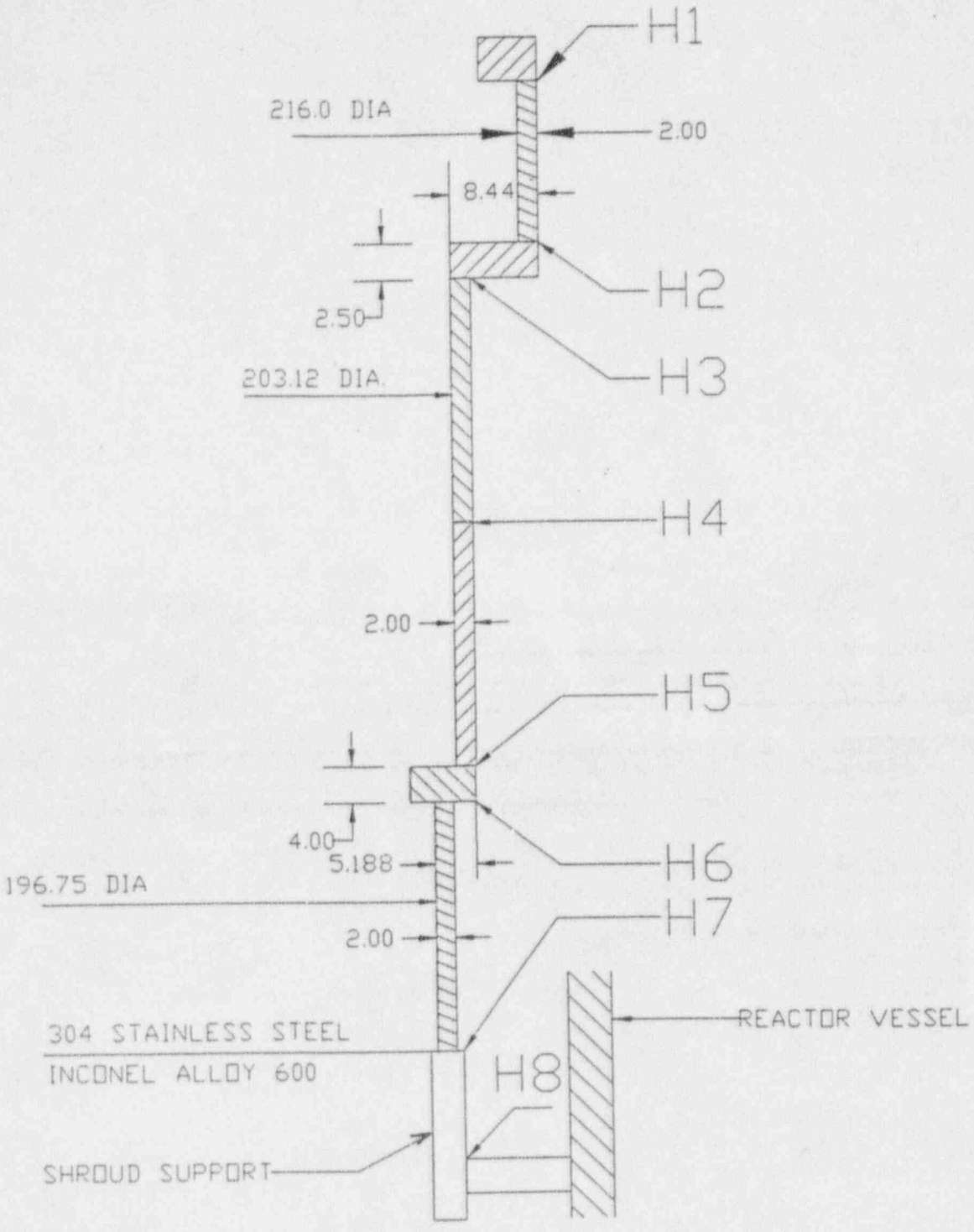

WELD NOMENCLATURE

FIGURE 2

GE RESPONSES

TO NRC QUESTIONS

FOR

PEACH BOTTOM SHROUD REPAIR

June 1995

CONTENTS

SHROUD SEPARATION AND THERMAL UPSET CONDITIONS

1. Introduction

The purpose of this document is to describe the analyses performed which evaluate the axial loading between the Peach Bottom shroud and the shroud repair stabilizers. The specific concerns to be addressed here are that of the potential of shroud separation during normal operating conditions with a shroud having all of the horizontal welds completely cracked and that of the potential for loss of preload due to plastic deformation of the stabilizers during a thermal transient event.

The method used to evaluate the axial loads in the stabilizer system was to determine the axial stiffness of the various components of the stabilizers and the axial stiffness of the various shells and rings of the shroud and to combine these using a finite element model with the effects of the appropriate temperatures, pressure differences and component weights. The resulting load balance of stabilizer tension and shroud compression demonstrates that the stabilizer tie rods maintain compressive loads at all of the shroud horizontal welds for the cracked shroud condition thereby assuring that the shroud rings and shells are held together and no separation occurs at the cracked horizontal welds. Additionally, the stabilizer components are shown to remain elastic and thus no loss of preload will occur for the axial loads in the stabilizer components which result from the uncracked shroud during a thermal transient event.

2. Description of the Analytical Model

This section presents a description of the analytical model and the inputs to the model which produce the axial load distributions in the stabilizer assemblies and shroud for the cases of normal operation with normal temperature and pressures and the case of a thermal transient with the corresponding temperature and pressures. The model is schematically shown in Figure 1. The model consists of a system of collinear two-dimensional beams, each beam representing the length and stiffness of a major component of the stabilizer assembly and shroud. Direct inputs to the beam elements of Modulus of Elasticity, coefficient of thermal expansion, temperature, distributed axial loading and point loads appropriately addressed the effects of component stiffness, temperature differences, pressure differences, component weights and mechanical preload of the tie rods. The ASIST computer program was used to solve the system of beam elements and produce the resulting load distributions.

2.1 Component Stiffness

The axial stiffness of each of the major components of the stabilizer and shroud system was determined by various methods depending upon the complexity of the individual structure. The stiffness was input to the beam elements of the ASIST model by means of an effective area that combined with the component's actual Modulus of Elasticity and length would produce the correct stiffness.

2.1.1 Stabilizer Axial Stiffness:
The axial stiffness of the lower stabilizer spring assembly and the upper support assembly were determined by finite element analysis. The tie rod axial stiffness was determined by a simple hand calculation of a beam in tension. The values used are shown in Figure 2.

2.1.2 Shroud Axial Stiffness:
The axial stiffness of the shroud was determined by a combination of finite element analysis and theoretical ring stiffness calculations. The axial stiffness of the shroud shell members, shroud support ring and struts were determined by finite element analysis. The resulting axial stiffnesses are shown in Figure 2.

The axial stiffness of the shroud shell to ring welded connection was determined using the method of analysis and equations from Section III, ASME B&PV Code, 1965 Edition, Appendix I, Article 1-2. This method was used for the ring axial stiffness between welds H2-H3 and H5-H6. The stiffness was determined for both the case of intact welds and fully cracked welds. The fully cracked welds were assumed to be through wall at the top of the weld fillet as schematically shown in Figure 3. Values of the axial stiffnesses used for the cracked and uncracked condition are shown in Figure 2.

2.2 Pressure Loads

The axial forces acting on the shroud due to reactor internal pressure differences were input to the ASIST model as point loads at the appropriate node location. Figure 4 shows the various pressure induced forces that were calculated. The force values are tabulated for both the normal operation and upset event pressure differences in Table 1.

2.3 Component Weights

The weights of the various components that provide axial loads on the shroud including the shroud weight itself were corrected for the effects of buoyancy and input to the ASIST model as either point loads or distributed axial loads along the beam elements. The values of the weights of the various components is summarized in Table 2.

2.4 Mechanical Preload

The mechanical preload that the tie rods exert on the shroud due to the initial installation torque of the tie rod nuts is directly accounted for in the ASIST model. The temperature value input to the tie rod beam member was adjusted to produce a length difference between the stabilizer assembly and the shroud at installation. The resulting length difference stretched the tie rod member the appropriate amount to produce the initial tie rod tension of 3346 Lb per tie rod.

3. Load Calculations

A sequence of five load cases was made with the ASIST model to produce the loads of interest. The sequence begins with the initial installation of the stabilizer assemblies onto a shroud that has all welds intact. Using the larger shroud stiffness for uncracked shroud welds will produce the maximum tie rod loads and stresses for the thermal transient condition. The shroud welds are then assumed to be fully cracked which reduces the shroud stiffness which produces a reduction in mechanical preload due to the stiffness change and produces the condition most likely to have shroud separation. The load values presented for each load case are the tie rod tension and the compressive load at shroud weld H6.

3.1 Load Case 1 - Stabilizer Assembly

The first load case is for the stabilizer assembled onto an uncracked shroud in the cold condition. Uncracked shroud stiffnesses are used, pressure forces are zero, all weights except the shroud head are applied and all temperatures are set to 70 °F. The tie rod temperature is then artificially reduced which creates tension in the tie rod system equivalent to the tension produced by the initial torque of the tie rod nut during assembly. The tie rod tension value is 3346 Lb and the compressive load at shroud weld H6 is 156,057 Lb.

3.2 Load Case 2 - Shroud Head Installation

This load case is identical to Load Case 1 except the shroud head weight is included as downward force. The net effect is to increase the compressive load at H6 to 277,657 Lb and reduce the initial tension in the tie rod to 962 Lb.

3.3 Load Case 3 - Normal Operation with Uncracked Shroud

This load case considers the uncracked shroud and stabilizer system in the hot operating condition with normal temperatures and pressures. Uncracked shroud stiffnesses are used, normal operation pressure forces from Table 1 and weights from Table 2 are input to the ASIST model. The temperature of the stabilizer components and shroud support members below H5 was set to 527 °F and the temperature of the shroud members above H5 was input as 539 °F. The resulting

tie rod load was 94,708 Lb and the compression load at shroud weld H6 was 65,564 Lb.

3.4 Load Case 4 - Thermal Transient Event with Uncracked Shroud

This load case considers the uncracked shroud and stabilizer system in the operating condition with upset pressures and temperatures from a thermal transient event combined to produce large tie rod tension in the stabilizer system. Uncracked shroud stiffnesses, upset pressure forces from Table 1, and weights from Table 2 were input to the ASIST model. The temperature of the stabilizer components was set to 300 °F and all members of the shroud and shroud support were input as 433 °F. The resulting tie rod load was 249,985 Lb and the compression load at shroud weld H6 was 500,112 Lb.

Each component of the stabilizer / shroud system was evaluated for stresses resulting from the 249,985 Lb axial load. The stress in each of the components was shown to be less than the material yield strength at the appropriate temperature thus assuring an elastic system with no loss of preload resulting from the thermal transient event.

3.5 Load Case 5 - Normal Operation with Cracked Shroud

This case is identical to Load Case 3 except the cracked shroud stiffnesses are used. The significant reduction in the stiffness of the system reduces the tie rod tension and compressive load at the shroud H6 weld, however, the shroud is maintained in compression by the tie rod stabilizers and no shroud separation occurs. The resulting tie rod tension was 79,343 Lb and the compressive load at shroud weld H6 was 4081 Lb.

Table 1
Pressure Forces Inputs to ASIST Model

Location	Normal ΔP, Psi	Transient ΔP, Psi
Lower Shroud	33.03	35.68
Upper Shroud	9.35	14.03
Core Plate	23.68	26.32

Force Location (Figure 4)	Normal ΔP Force (Lb)	Transient ΔP Force (Lb)
F1	109,150	117,910
F2	96,430	104,160
F3	423,910	457,920
F4	12,180	12,190
F5	130,140	130,280
F6	39,630	59,460
F7	12,570	18,870
F8	6,260	9,390
Shroud Head	336,310	504,630

Table 2
Weight Inputs to ASIST Model

Component	Weight in Cold Water (Lb)	Weight in Hot Water (Lb)
Shroud Head	131,136	136,042
Shroud	99,761	103,494
Core Spray	1,751	1,817
Top Guide	18,118	18,796
Core Plate	27,182	28,199
Peripheral Fuel Supports	231	240
Peripheral Fuel Bundles	13,272	13,728

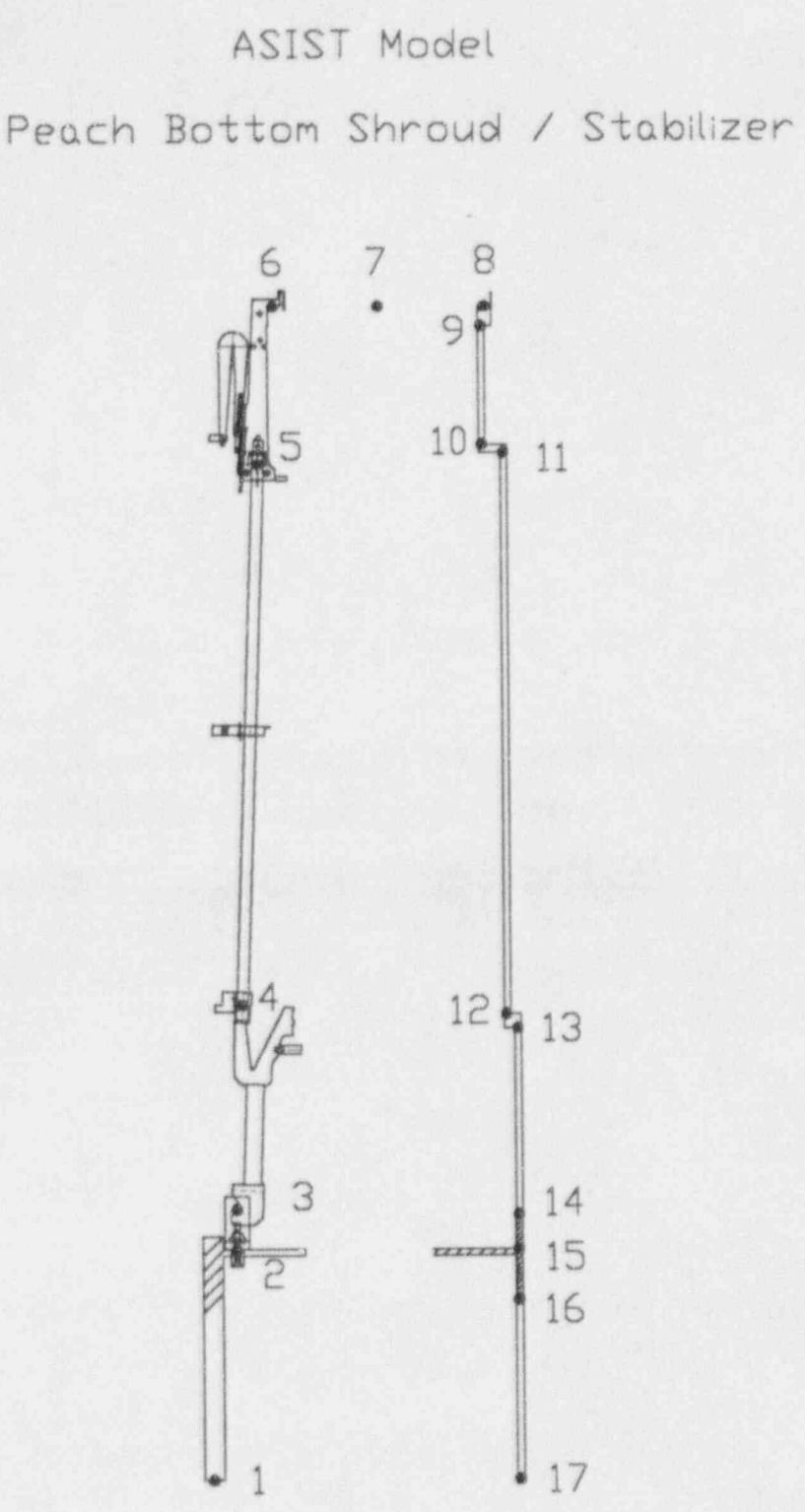

Figure 1. Peach Bottom Shroud / Stabilizer ASIST Model Definition

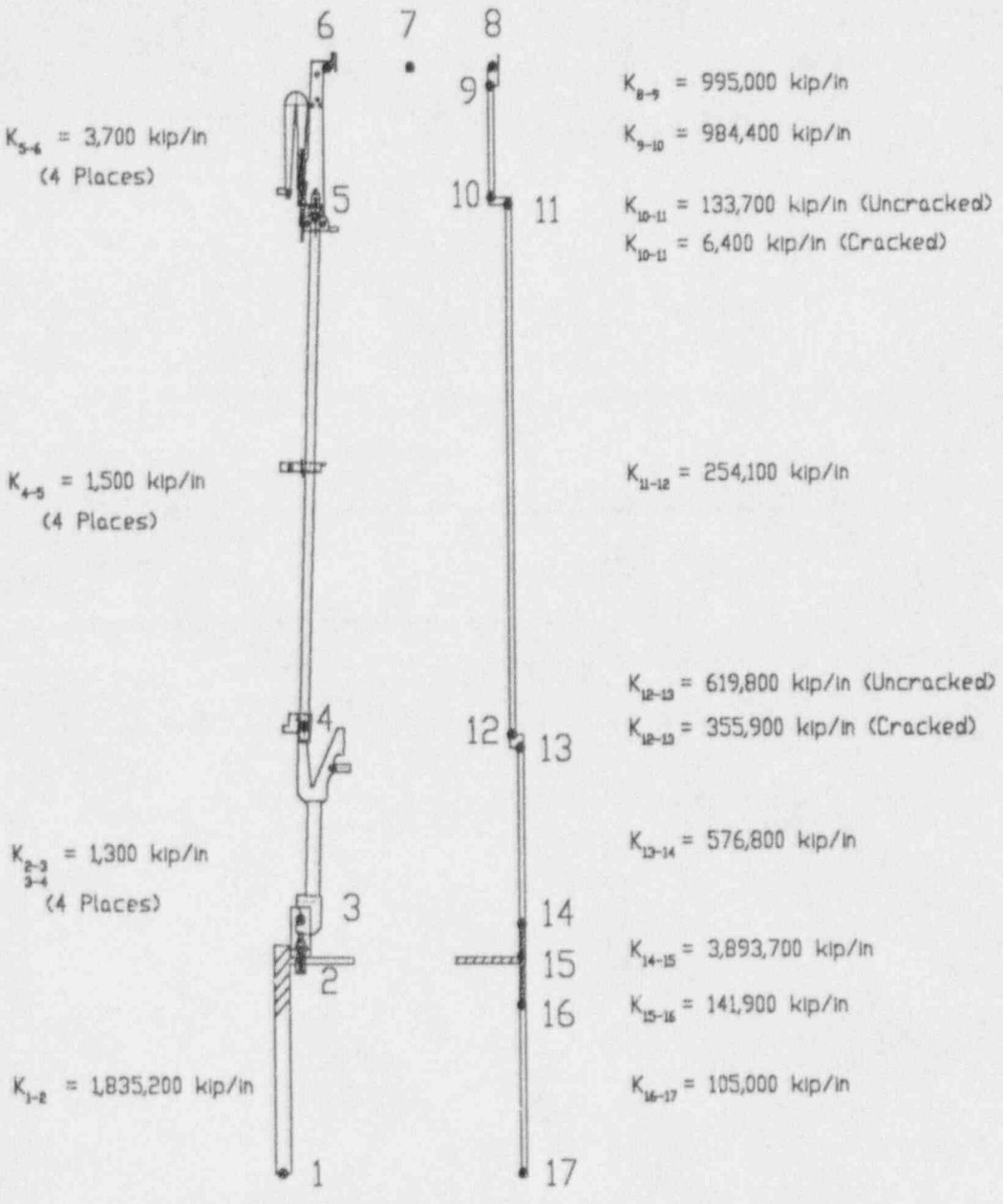

Figure 2. Peach Bottom Shroud / Stabilizer
ASIST Model Axial Stiffness Values

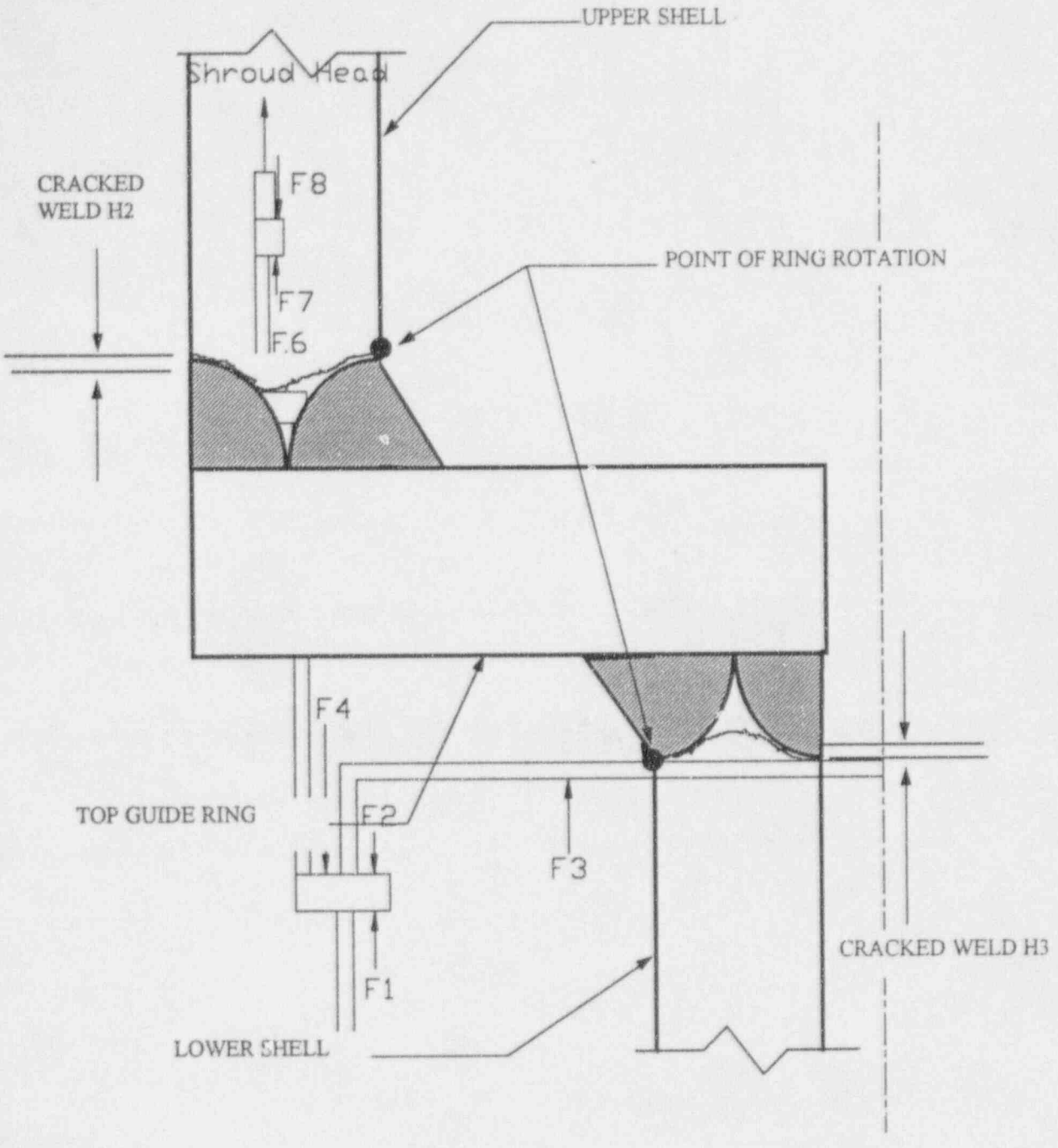

FIGURE 3
RING ROTATION ABOUT TOP OF FILLET
(NOT TO SCALE)

Seismic Analysis

Introduction

The information provided below are a selection of Seismic related questions asked by the NRC about the shroud repair installation. These seismic questions with their appropriate responses to the NRC were selected from the NRC questions and GE prepared responses for Nine Mile Pt. 1, Quad Cities, Hatch 1, and Pilgrim shroud repair projects.

Seismic Analysis/Methods, Input, & Results

The seismic analysis with shroud repair hardware installed, and with numerous combinations of cracks at welds H1 through H8, was performed by time-history method. The peak responses from these seismic analysis were used to obtain loads and deflections in the shroud, the shroud repair hardware and the RPV & RPV internals for use in subsequent stress analysis. The NRC questions address the subjects which are listed below:

1. Seismic analysis methodology including request for copies of Criteria & computer program User's Manual.
2. Seismic Model details.
3. Seismic Input details.
4. Maximum gaps calculations at cracks with seismic loads included.
5. Seismic analysis results details / explanations.

Following is the grouping of questions into the above FIVE topics.

Topic # 1

Seismic analysis methodology including request for copies of Criteria & computer program User's Manual.

Question # 1

Provide Reference 2 of GENE-771-60-0994 (GE document NEDO-10909,Rev. 7, December 1979,SAP4G07 Users Manual) which discusses the "standard, strain-energy weighted modal damping ratios."

Response # 1

The reference document is a Users Manual for computer program used by GE in performing the seismic analysis. This document is available in NRC offices because it was provided as part of ComED's March 3, 1995 submittal. Therefore, it is not submitted as part of Peach Bottom submittal. See page VIII.L-4 of the manual for the related details applicable to this question.

Question # 2

It is stated that the component stress evaluations are determined from the dynamic analysis of the horizontal seismic loads in combination with the vertical seismic loads. How were the horizontal and vertical loads combined (i.e., by absolute summation or by another method), and how were they combined according to the original plant design basis? Similarly, how were the SSE and LOCA dynamic loads combined for the two faulted service conditions, and how were they combined in the original design of the core shroud?

Response # 2

There are three possible collinear contributions for each seismic load. One for each of the two horizontal components of seismic excitation and one for the vertical. For the Peach Bottom shroud repair hardware design, the maximum contribution from either of the two horizontal seismic analyses was combined absolute sum with the corresponding peak vertical contribution for each seismic load "See GENE-771-60-0994". This method for combining peak collinear contributions due the three orthogonal spatial components of excitation is identical to the original (and existing) licensing design basis for Peach Bottom.

Also, commensurate with the primary structure being vertically rigid with respect to the vertical seismic free-field input motion, the Peach Bottom seismic licensing design basis necessitates only horizontal dynamic analyses. Consequently, in conjunction with existing geometric symmetry in the primary structure, the peak horizontal components were obtained from separate N/S and E/W horizontal analyses and the peak vertical contributions were from static dead weight analyses.

The peak collinear contributions due to the SSE and LOCA dynamic loads were combined by absolute sum for the Peach Bottom shroud repair hardware design. It is not clear how they were combined in the original design of the core shroud. However, the absolute sum methodology presently used is the most conservative method employed for nuclear application.

Topic # 2

Provide seismic model details such as core data, rotational spring constants, including their derivations, how a hinge or roller condition at cracks is determined as well as modeled.

Question # 1

Provide the differences between the original core configuration and the Cycles 11 (Unit 2) & 10 (Unit3) core configuration

Response # 1

Both the original and Cycles 10 & 11 core configurations contain 764 fuel bundles in each unit. The differences between the two core configurations are summarized below.

	Original Core	Cycle 11 Core	Cycle 10 Core
		Unit 2	Unit 3
Young's Modulus (ksf)	1.67E6	1.59E6	1.59 E6
Poisson's Ratio	0.30	0.41	0.41
Total Shear Area (ft2)	4.48	3.99	4.30
Total Moment of Inertia (ft4)	0.285	0.268	0.286
Total Fuel + Water Mass (k-sec2/ft)	16.4	15.22	15.58

Both the stiffness and mass of the Cycles 10 and 11 cores are smaller than those of the original core. The revised Cycles 10 and 11 core properties were included in the seismic analyses used for the design of the shroud repair hardware

Future core configurations are not expected to be significantly different from the Cycles 10 & 11 core configurations and, hence the seismic loads in the restraint hardware and the RPV/internals are not expected to be sensitive to future changes in the core configurations.

Question # 2

Provide Reference 1 (GE Document 383HA691, Rev. 0, Peach Bottom Units 2 &3 - RPV and Internals Seismic Analysis, April 6, 1972).

Response # 2

The reference is provided as Attachment A.

Question # 3

Provide the detailed calculation of the rotary spring constant K4 for both an uncracked and cracked weld H8, and indicate how it is introduced in the analysis.

Response # 3

The Peach Bottom Core shroud is physically supported by a shroud support plate and six vertical shroud support legs. The shroud support plate is an annular plate with its outer edge welded to the vessel wall and its inner edge welded to the shroud support ring. The plate also serves as a support for the jet pumps. The shroud support legs are steel bars of rectangular cross-section.

The vertical legs are connected in uniform circumferential spacing between the bottom of the shroud support ring and the vessel bottom head.

Considering the moment resistance characteristics of the design configuration and the fact that the primary structure seismic model is a mathematical beam element model, the shroud support hardware is modeled as a rotational spring (K4). Both the shroud support plate and the support legs contribute to the total stiffness of the K4 spring. The rotational stiffness of the two parts are computed separately, and the total K4 stiffness is the summation of the two.

For the shroud support plate, the rotational stiffness is derived using the appropriate moment-rotation resistance equation representing a fixed-support annual ring by applying a moment to a central rigid circular block. The reduction in plate area due to the jet pump holes are also taken into consideration in computing the equivalent plate stiffness. For the shroud support legs, the axial stiffness of the individual legs is computed first. The rotational stiffness is derived by a moment-rotation relationship considering stiffness contributions from support legs placed at proper geometrical locations around the bottom of the shroud support ring. For a total rotational stiffness K4 of Peach Bottom, the rotational stiffness contributions from the support plate and support legs are, respectively, about one-tenth (10 %) and nine-tenth (90 %) of the total stiffness value.

The H8 weld is the weld that connects the shroud support plate to the shroud support ring. When H8 has a full 360 degree through-wall crack, the worst case will result in no rotational coupling between the support plate and the shroud. However, since the support plate only contributes about 10 % of the total rotational stiffness for K4 spring, there is still at least 90 % of the rotational stiffness remaining to resist the seismic responses. As compared to the other crack cases, which assume full 360 degree through-wall cracks in the shroud wall, the H8 crack is not a controlling case in the shroud safety evaluation nor in the shroud repair hardware design. The reduction in the stiffness of the shroud support by approximately 3 % is a much less severe case than either the hinge or roller cases assumed in the design of the shroud repair hardware and thus is adequately enveloped by the various parametric analysis performed.

Question # 4

Clarify the basis and conditions under which the assumption of hinges or rollers is chosen to model the shroud. Provide detailed diagrams of the hinge and roller models of the shroud structure, showing the attachments to the RPV. For each loading combination and crack configuration state the model which was used in the analysis.

Response # 4

A hinge was chosen to model a 360 degree through wall circumferential crack in the shroud when contact is maintained under a compressive load, based on mechanical interference at the crack resisting lateral motion. A roller was chosen to model a crack when sufficient pressure and seismic loads exist to overcome the mechanical and thermal preloads and dead weight such that the full crack surface may open up, losing mechanical interference. This only occurs for the main steam line LOCA in combination with a MCE. Note that the results of the parametric study were used to determine the location of the crack that produced the largest response for the shroud and the shroud stabilizer hardware.

The detailed seismic model is shown in Figure 1 of the GE Document GENE 771-60-0994, Revision 2, "Peach Bottom Units 2 & 3 Seismic Analysis. Two coincident nodes are modeled at each shroud circumferential weld location; one attached to the upper beam element, and one attached to the lower beam element. If there is no crack, the nodes are coupled in both translation and rotation. If there is a crack which is modeled as a hinge, the nodes are coupled in translation only, with no moments transmitted through the nodes. If there is a crack which is modeled as a roller, the nodes are uncoupled, with no shear or moment transmitted through the nodes.

For the design basis load combinations of DBE plus normal condition, and the MCE plus normal condition, assumed weld cracks are always modeled as hinges, since for the normal operating conditions a preload is always maintained. For the beyond design basis load combination of MCE plus recirculation line LOCA condition, the assumed weld cracks are always modeled as hinges, since for this condition a preload is always maintained. For the beyond design basis load combination of MCE plus main steam line LOCA condition, with a single crack (critical bounding location assumed), the crack is modeled as a roller, since the uplift forces overcome the preload. For the MCE plus main steam line LOCA condition, with multiple assumed cracks, all cracks are modeled as hinges except for the topmost crack which is modeled as a roller. In this case, the uplift forces overcome the preload for the topmost crack, while the deadweight of the lower portion of the shroud is sufficient to keep the remaining cracks closed (i.e. pinned condition).

Topic # 3

Seismic model input details

Question # 1

Describe how uncertainties were accounted for in the structural model and the time-history input.

Response # 1

The purpose in addressing the effects of parameter variations is to account for uncertainties in the calculated natural frequencies due to uncertainties in such parameters as material and soil properties, structural damping and soil damping, soil-structure interaction techniques, geometrical dimensions and approximations inherent to dynamic modeling and analysis. The concern is the effect the parameter variations will have on response of the RPV and internals.

The current NRC acceptance criteria for the consideration of the effects of parameter variations are provided in Subsections II.9 and II.5 of Standard Review Plan (SRP), Section 3.7.2, "Seismic System Analysis", Rev. 2 - August 1989. Per the SRP, one acceptable approach is to smooth the computed floor response spectra obtained from the primary structure time history analyses and broaden the spectral peaks that are coincident with the structural natural frequencies for subsequent use in decoupled secondary system analyses. Also, from Subsection II.5 of SRP 3.7.2, it is acceptable to use a "single" artificial input time history (without expanding or contracting the time history time step) in the primary structure seismic analysis. However, since the original design basis seismic analysis in UFSAR did not require applying these criteria, the current analysis does not specifically document compliance with these criteria even though, the intent of Subsection II.5 of SRP 3.7.2 is met.

For the Peach Bottom shroud repair, a coupled model time history analysis was performed in which the reactor and internals are modeled in detail in the primary structure model. Key input parameters such as the rotational stiffness of the tie rod assemblies along with the various crack locations and joint restraint configurations were parametrically evaluated by performing analysis of bounding conditions. Conservative peak dynamic loads were then calculated in the primary structure analysis; without the need for a separate secondary system analysis procedure.

Two separate time histories (DBE and MCE) were used in the primary structure time history analyses for the seismic design adequacy evaluation of the shroud repair hardware. Time history analyses were performed using both of these synthetic time histories. Synthetic acceleration time-histories were constructed for both DBE and MCE in accordance with the guidelines in the USNRC Standard Review Plan (NUREG-0800), such that the response spectra corresponding to the synthetic time-history envelopes the spectra of Figures C.3.1 & C.3.2 of Peach Bottom UFSAR. The UFSAR spectra (Target spectra) and the spectra corresponding to the synthetic time-history used in the current analysis are shown in Figure 2 of the seismic report GENE-771-60-0994, Rev. 2.

Finally, it is noted that only the peak bounding dynamic loads from the Peach Bottom time history analyses were applied to perform the static stress analyses

of the shroud and shroud repair hardware, and thus no secondary subsystem analysis was required.

Topic # 4

Provide Maximum gaps calculations at cracks with seismic loads included.

Question # 1

Provide the magnitude of the maximum separation of each cracked weld during a MSLB plus vertical seismic loading.

Response # 1

The magnitude of the maximum separation at a cracked weld during a MSLB plus the Maximum Credible Earthquake considering vertical seismic excitation will be 0.30 inches.

Topic # 5

Provide seismic analysis results details such as a few mode shapes & modal dampings for uncracked, the hinged and the roller models; RPV loads etc.

Question # 1

Provide a detailed discussion of the difference between the seismic axial and bending loads in the original skirt stress analysis report and the present analysis.

Response # 1

The bending moments in the original analysis and present analysis are of the same nature, but have different numerical values as noted in Section 4.9 of the present stress report. The original bending moments were calculated based on the seismic horizontal design acceleration coefficient of 0.6 g(in DBE) and 0.12 g (in MCE) and taking the summation of the moments of the horizontal seismic loads located at the center of gravity (C.G.'s) of each load causing overturning moments. This was given in GE Drawing 886D499, sheet 7, Revision 8, table 10 for the original analysis. This drawing is being provided as Attachment B.

In the present analysis the bending moments are taken directly from the dynamic analysis of the seismic model, the details are available in GENE-771-60-0994, Revision 2, which is included in this submittal. This analysis was performed using time-history methodology.

The original seismic axial load was based on a vertical acceleration coefficient (=0.08g DBE & 0.16g MCE) multiplied by the total downward load. This axial load has not been changed in the present analysis.

Question # 2

Provide the detailed calculation showing that the shroud legs have been checked for buckling with H8 cracked under preload and vertical and horizontal seismic loading.

Response # 2

The original compressive stress in the shroud support legs using conservative design (DBE)loads is 12.1 ksi, which is below the allowable of 14 ksi (= 0.4 Sy) thus meeting the buckling stress limits. The new compressive stress in the shroud support legs for MCE is 22.9 ksi, which is below the allowable of 28 ksi (= 0.8 Sy). Since the revised seismic moments from the seismic time history analyses on the shroud support legs are lower than those used in the original analysis, the existing buckling stability evaluation documented in the original stress report is still valid. The new loads are from the case of H8 uncracked but are the same for the H8 cracked case.

Question # 3

Provide the number of modes, the first five modal shapes and the corresponding modal damping values, for the uncracked, the hinged and the roller models.

Response # 3

The seismic analysis included all modes with modal frequencies less than 33. Hertz. Shown in the following tables are the number of modes, the first five modal frequencies and composite modal damping ratios along with the identification of the location of the predominate mass by mode. Provided in Figures 1, 2, and 3 below are the first five mode shapes for the uncracked model, a representative hinged model (weld H7 cracked as a hinge), and a representative roller model (weld H7 cracked as a roller). Because of similarity in modal properties between the East-West and North-South direction, it is sufficient to show only the modal properties in the North-South direction. Note that for most of the internal components the N-S model produces the bounding responses.

Uncracked (22 modes)			H3 Hinge (22 modes)			H3 Roller (23 modes)		
Freq. (Hz)	Damping (% crit.)		Freq. (Hz)	Damping (% crit.)		Freq. (Hz)	Damping (% crit.)	
3.64	2.00	(2)	1.66	1.12	(1)	1.08	2.04	(1)
4.34	6.07	(4)	3.64	2.00	(1)	3.02	2.18	(1)
5.25	3.48	(3)	4.87	6.65	(4)	3.64	5.02	(2)
5.89	2.06	(2)	5.25	3.49	(3)	5.24	3.50	(3)
7.17	1.74	(1)	5.89	2.02	(2)	5.54	6.63	(4)

Predominant Response Location Legend

(1) Shroud, Fuel
(2) Reactor Building Roof Structure
(3) Control Rod Drives
(4) Fuel

Figure 1
Mode Shapes for Uncracked Case

Figure 2
Mode Shapes for H3 Hinge Crack Case

Figure 3
Mode Shapes for H3 Roller Crack Case

ATTACHMENT A

GE Document 383HA691, Rev. 0, Peach Bottom Units 2 & 3 - RPV and Internals Seismic Analysis, April 6, 1972.

ATTACHMENT B

GE Drawing 886D499, Sheet 7 of 8, Revision 8

GENERAL ELECTRIC INSPECTION RECOMMENDATIONS

FOLLOWING THE INSTALLATION OF THE SHROUD STABILIZERS

AT PEACH BOTTOM 2, 3

GE Nuclear Energy recommends that the following in vessel inspections be performed after the installation of the shroud stabilizer assemblies at Peach Bottom Unit 2 or Unit 3. The complete inspection recommendations are not yet finalized, and will depend in part on the criteria established by the BWRVIP.

Perform a VT-3 visual inspection of each shroud stabilizer assembly and interfacing areas on the shroud and vessel after one operating cycle, and once per interval thereafter. This inspection should include verification that the crimp nuts on the toggle bolts, and other locking devices are in place. The inspection should include the interface locations between the stabilizers and the shroud and reactor pressure vessel. The anchor points at the shroud support plate, lower spring and clevis pin should be included to verify structural rigidity. It is not considered necessary to mechanically check the tie rod nut torque.

Perform an enhanced VT-1 visual inspection or UT inspection of each of the four vertical shroud welds at the intersection with the H4 weld once every two fuel cycles or after every three years, whichever is longer. A minimum length of eight inches should be inspected for each weld. It is not considered necessary to inspect the remaining vertical welds which do not intersect the H4 weld.

Follow the BWRVIP plan for the inspection of the H9 weld between the shroud support plate and the vessel, and any recommendations for inspection of the shroud support plate segment welds. An analysis for maximum allowable flaws in the H9 weld would help determine inspection criteria.

There is no inspection required for the top guide support ring (between the H2 and H3 welds), and the core plate support ring (between the H5 and H6 welds) as these are one piece rings without any welded ring segments.

There is no recommended inspection for the H8 weld between the shroud support plate and the shroud support cylinder as it has been shown by analysis that the structural integrity of the H8 weld is not required by the shroud stabilizers.

Materials

Introduction

The information provided below are a selection of material related questions asked by the NRC about the shroud repair installation. These material questions with their appropriate responses to the NRC were selected from the NRC questions and GE prepared responses for Nine Mile Pt.1, Quad Cities and Peachbottom shroud repair projects.

Shroud Repair Materials

The shroud is fabricated from 304 series stainless steel. The shroud repair hardware is fabricated from three (3) types of materials which are listed in the Peachbottom fabrication specification 25A5601 Rev 1. These repair hardware materials are;

1. The X-750 is a nickel-chrome-iron (Ni-Cr-Fe) alloy shall be in accordance with ASTM E-637, UNS N07750, Type 3 with additional requirements as defined in paragraph 3.2.1 of the fabrication specification.

2. The austenitic 300 stainless steel shall be in accordance with ASTM A-479, A-182 or A-240 type 304, 304L, 316 or 316L with a maximum carbon content of 0.020 percent with additional requirements as defined in paragraph 3.2.2 of the fabrication specification..

3. The XM-19 stainless steel shall be in accordance with ASTM A-479, A-182 or A-240 with a maximum carbon content of 0.040 percent with additional requirements as defined in paragraph 3.2.3 of the fabrication specification.

Subjects Addressed By NRC Material Questions

The NRC questions address the follow subjects and are listed below.

* Details of heat treatment
* Sensitization testing
* Cold work during fabrication
* Lubricant used during installation
* Use of XM-19 material for tie rods
* Certified Material Test Reports (CMTR)

Selected NRC Questions

Listed below are a selection of material questions asked by the NRC during the review of the documentation submitted for Nine Mile Pt.1, Quad Cities and Peachbottom shroud repair projects for additional information. GE reviewed each NRC question and submitted the appropriate response for each material question.

Question 1

Please provide the heat treatment details such as time, temperature and cooling rate that are specified for the alloy X-750 components.

Response 1

Heat treatment for the X-750 consists of 1975° ± 25° for 60 to 70 minutes, followed by forced-air cooling. Age hardening is done at 1300 ± 15° F for 20 to 21 hours, followed by air cooling.

Question 2

Is solution annealed condition specified as the final material condition for all components made of XM-19 and 316 or 316L austenitic stainless steel materials?

Response 2

Solution heat treatment is required for all 300-series and for XM-19 parts. This is done before machining and trimming. Threads on the XM-19 tierods are not annealed after machining.

Question 3

What is the material condition of XM-19 that were previously used in the BWR environment?

Response 3

This material was selected for the shroud-reinforcement-assembly tie rods because of its strength, corrosion resistance in BWR environments, and other engineering properties.

As purchased, this material is delivered in the solution heat treated condition. This involves heating the item into the temperature range, approximately 2000° F for UNS S20910, where the $Cr_{23}C_6$ carbides break down and the component atoms disperse into the matrix. This heating is followed by cooling at a rate rapid enough to maintain the dispersion in the matrix.

For some materials, and for small parts, the rapid cooling is most conveniently achieved by quenching in a water bath. But for the stock for shroud-restraint tie rods, which are approximately 3-1/2 inches in diameter by 14 feet long, attempts at water quenching will introduce severe local distortions because the

entire length of such an object rarely, if ever, reaches the same temperatures at the same times. Therefore, air cooling was selected to reduce the likelihood of problems due to nonuniform temperature distribution.

For this specific alloy, air cooling is sufficiently rapid to avoid reprecipitation of carbides, as has been verified by a number of laboratory tests and experiments. For example, data published by EPRI's M. J. Povich and D. E. Broeker in the October 1979 issue of *Materials Performance* (National Association of Corrosion Engineers; "The Stress Corrosion Cracking of Austenitic Stainless Steel Alloys in High Temperature Air Saturated Water") show that UNS S20910 is as resistant to corrosive attack in the cold-worked and/or furnace-sensitized condition as in the fully solution-heat-treated condition. Therefore, for parts of the size, shape, and basic material of the tie rods, more is to he lost than gained from water cooling after solution heat treatment. Air cooling is sufficiently rapid to preserve the corrosion-resistant properties of the material without the risk of unacceptable loss of straightness.

This, and other similar data in the literature, also supports the decision to place the completed tie rods into service in the as-machined condition, without incurring the schedule delays and added expenses that would have resulted from an unnecessary post-machining heat treatment cycle.

Question 4

In the fabrication specification, GE stated that the successful completion of the sensitization testing shall be accepted as evidence of the correct solution heat treatment if time and temperature charts are not available. The staff considers that in a good quality assurance program, accurate records of item, temperature and cooling rate are necessary to be maintained as evidences that proper heat treatment has been performed. Therefore, the use of sensitization test results as a substitute for the proper heat treatment documentation is not acceptable.

Response 4

The purpose of the requirements on heat treatment of stainless steel core shroud repair materials is to provide material that is not sensitized. Accordingly, sensitization testing of the material after heat treatment is an accurate indicator that the heat treatment was effective. The attributes of the final material condition is considered as evidence that the engineering requirements of material performance have been met. Therefore, sensitization testing is considered an adequate alternative to detailed heat treatment records in assuring that proper heat treatment has been performed. Also, complete reliance on heat treatment records can be misleading. GE has indicated that isolated cases have occurred in which heat treatment details were recorded, even to the extent of using embedded thermocouples, but that the subject material failed to pass a sensitization test.

ASME NCA-3800 was followed to procure the core shroud repair material. With respect to material test reports, NCA-3860 does not require that detailed time/temperature records for heat treatment be recorded but that specific time and/or temperature parameters be recorded if such values are specified in the underlying Section II material specification. For the austenitic stainless steels used for the shroud restraints, the only stated requirement is a minimum temperature of 1900 degrees F (followed by rapid cooling).

The fabrication specification adds additional requirements for heat treating stainless steel that is over and above the ASME code. When material is ordered in heat lots from a primary melter, it is possible to get such detailed records of heat treatment. However, in the current environment of performing internals repairs, materials are procured in small quantities, often from a third party supplier out of a warehouse inventory. In these cases, detailed records showing complete conformance to the additional requirements are not always retrievable. It is in these cases where, as an alternative to detailed heat treatment records, the attributes of the final material condition is considered as evidence that the engineering requirements for materials performance have been met.

In summary, the material ordering requirements are appropriate for the intended use and are in conformance with applicable codes.

Question 5.

General Electric stated that a minimum of 0.030 inches of austenitic 300 series stainless steel materials will be removed after high temperature annealing as a control of intergranular attack (IGA). Will this process or any other process be applied to machined threads made of XM-19 and Alloy X-750 after high temperature annealing to ensure there is no IGA.

Please provide test data to support that the removal of 0.030 inches surface material would effectively eliminate the IGA effect resulting from the high temperature annealing.

Response 5.

Material removal processes are not used on the XM-19 tie rod threads after the final machining. The minimum of 0.030-inches to be removed after annealing or high temperature heat treatment of 300 series stainless steel, XM-19 and Alloy X-750 is intended to address parts which may be in an air atmosphere furnace for several hours. At temperatures of 1800-2000 degrees F, in air for several hours a thick surface oxide layer and grain boundary oxidation (IGA) may occur.

The local solution annealing of the threads is a very short cycle with very short heat up and cool down times. Considering the outstanding corrosion and oxidation resistance of XM-19, it is expected that the oxidation of the surface

will not be of a significant depth, and IGA is not expected during this very short process. Therefore, no material removal processes are used on the XM-19 tie rod threads after the local induction annealing.

Re-solution anneal or additional material removal processes are not performed on X-750 parts after machining. Typical UNS N07750 (X-750) samples were selected at random from their actual production runs, cross-sectioned, and the microhardness measured as a function of depth into the metal from the polished surface. The sequence of manufacture was:

Sample "A"	Sample "B"
Machined	Age Hardened
Polished	Machined
Age Hardened	Polished
Penetrant Examined	Penetrant Examined
Dimensions Checked	Dimensions Checked

In both specimens, the hardness at and near the polished surfaces was identical to that of the unaffected interior: Rc 36 for "A" and Rc 35 for "B". All readings remained within a plus or minus 3-point tolerance band, which is uniform and consistent for 100-gram Knoop readings. The surface showed no evidence of work hardening or cold work. Additionally, samples representing turning and milling operations on X-750 after age hardening showed no significant increase of surface hardness compared to internal bulk hardness (38Rc max surface verses 34Rc interior). Therefore, no re-solution anneal is required for X-750 parts after machining.

Over the past 25 to 30 years GE has implemented a metallographic receipt inspection requirement for heats of stainless steel. The receipt inspection requirements consist of a destructive metallographic examination of the cross section from each heat to determine the depth of IGA that may have occurred due to high temperature annealing atmosphere or due to an overaggressive acid pickling process. The acid pickling process is the primary cause of IGA The results of the numerous tests performed have shown that less than one sample per year have shown IGA deeper than 0.001 inch and in those cases the depth of the IGA was less than 0.003 inches.

The criteria for removal of 0.030 inches of material was originally established many years ago to be a conservative bounding limit to ensure that any IGA induced by any process, especially due to overaggressive pickling, would be removed. This criteria was established based on engineering judgment prior to the results of the material receipt inspection testing as described above. The requirement for removal of 0.030 inches from the affected surfaces has been

implemented for this project to provide an order of magnitude of the margin over the maximum depth of IGA that has been observed.

Question 6

Provide details of your controls in the practices of machining, grinding and threading to minimize the effect of cold work, such as amount of material to be removed in each pass, application of coolant and sharpness of the tool.

Response 6

The amount of material removed in a single pass depends on the part and the particular machine doing the work. Parts are generally rough machined to within 0.10" of final size and skim passes are used to achieve the final dimensions. Tests show that Inconel X-750 surfaces are unaffected by machining and do not require heat treatment. The application of coolant and sharpness of the tool is considered adequate provided a surface finish of 125 root mean square or better is obtained.

Question 7

Please provide details of your controls in the practices of machining, grinding and threading to minimize the effect of cold work, such as amount of materials to be removed in each pass, application of coolant and sharpness of the tool.

Response 7

Each item that is manufactured has its own specific requirements when it comes to "how much" material is removed per pass and which machine is doing the work. Generally speaking, parts are "rough machined" down to within .100" of final dimensions. Then the final clean up (about .010") pass skims off the required amount of material to achieve the required size and surface finish. If a tool is dull, then the 125 rms surface finish would not be produced as required on all drawings. A dull tool produces a smeared or torn surface appearance which is the primary method of monitoring the adequacy of the tooling and the process in general.

The judgment and experience of the machinist is relied upon to determine how much material can be safely removed per cut or per pass. Written documents could not possibly address all possible eventualities of workpiece size, shape, and material or machine type and capacity or dimensions, tolerances, and surface finish necessary. Vendor in process control sheets or travelers are used to control the flow of material in the shop. While in process, machining is seldom, if ever, controlled by fixed documents. The end results are carefully specified on the drawings.

In addition, the fabrication specification states " Machined components that are not solution annealed after machining shall have metallographic and microhardness evaluation on test samples. Samples shall be provided from the same material, same fabrication shop and using the same process variables."

The purpose of these evaluations is to verify the materials' surface conditions have very shallow cold work depth. Control of the cold work depth will minimize the materials susceptibility to IGSCC.

The coolant used during the machining process is Trim-Sol. A stream of Trim-Sol is applied directly to the cutting tool where it makes contact with the part. Afterward, the component is washed with acetone and followed by a demineralized water wash prior to any other operation.

Question 8

In your fabrication specification it is stated that ,if grinding is not followed by solution heat treatment or machining, the grind surface shall be polished to an RMS 32 finish or better using successively finer grit abrasive. Please provide test data to support the above stated polishing to be effective in eliminating the unacceptable surface cold work resulting from grinding

Response 8

The fabrication specification was based upon several evolutions of shroud-reinforcement documents and has retained several contingency options that at earlier times were thought to be prudent to have available "just in case". Shaping metal by heavy grinding was one of these options. Experience now shows that such a technique is not necessary and, in fact, has not been used.

While experiments have been conducted to verify the metallurgical acceptability of the manufacturing operations that we do use or intend to use, no specific tests were made of 'heavy grinding with and without subsequent polishing'. Thus there are no test data available to be provided on this specific phenomenon

Question 9

In the fabrication specification it is stated that electropolishing can be specified to remove any cold-worked surface by using mixed phosphoric/sulfuric acid. Please describe the details of the electropolishing process and its controlling parameters, as well as how this process was qualified. Is there any test requirement after electropolishing to ensure that there is not pitting or IGA on the electropolished surface?

Response 9

Electropolishing to remove surface material for elimination of mechanical-working effects, refinement of surface texture, fine adjustments to dimensional attributes, or similar reasons; is permitted under the following mandatory requirements:

a) All work shall be performed in accordance with written and approved procedures, Such documents shall control, as a minimum: basic electrolyte composition with limits, maximum permissible bath

contaminants by type and level, immersion temperatures with limits, current polarity and maximum amperes/cm^2 density, precleaning and postcleaning requirements, and limitations to preclude insufficient or excessive material removal.

b) The electrolyte shall be based upon the mixed phosphoric/sulfuric acid system, with appropriate buffers and/or intensifiers permitted.

c) Demonstration samples shall be prepared and submitted for information in conjunction with the written procedure (subparagraph (a) above). These shall clearly show the alteration in surface texture and appearance after electropolishing and compared with before electropolishing, and shall include polished and etched metallographic cross sections of before and after specimens to illustrate typical internal structures.

Question 10

Please discuss the mitigation methods that you plan to apply to the machined threads such as re-solution annealing to minimize the cold work effect. Please also describe how the methods were qualified and the details of controls for application.

Response 10

The XM-19 material used for the tierods is procured in the solution annealed condition. The machined threads on the tierods are not solution annealed after the machining of the threads.

General Electric has been specifying and using XM-19 components in commercial power reactors since the mid-1970s, especially for parts which must be stainless steel and also must be nitrided. The nitriding process involves holding the parts in a chlorine-rich nitrogen environment at 1060° to 1100°F for 16 to 24 hours. Only XM-19 is able to withstand this treatment without becoming sensitized to Intergranular Stress Corrosion Cracking (IGSCC). Types 304, 304L, 316, and 316L quickly fail after exposure to such thermal conditions, but not XM-19. Therefore it is not necessary to remove or anneal any "IGSCC-prone" surface layers after machining, because the material is inherently resistant to IGSCC, even in the as-machined condition.

GE has access to test results which show that XM-19, in BWR environments, is more corrosion and crack resistant in tight crevice situations than 316L or other 300 series stainless. To cite an example; a set of tensile specimens, each bearing a sleeve to create a crevice at the specimen surface, was loaded to 120% of yield in 1981 and that load maintained for the duration of the test. Today, 14 years later, none of the XM-19 specimens has failed or even cracked. Thus, concerns about the durability of XM-19 in threaded joints because of "crevices" are not valid.

All in all, XM-19 is an excellent material for use in BWR applications. It may safely be used in the as-machined condition; it may safely be used in threaded and other highly-creviced geometries, and is superior to 316, 316L, and other alloys for the intended application. Its only drawback is cost and availability - it is not as commonly found in supplier's inventories as the more traditional materials.

Question 11

Please provide details of your controls in the practices of machining, grinding and threading to minimize the effect of cold work, such as amount of materials to be removed in each pass, application of coolant and sharpness of the tool.

Response 11

Each manufactured piece has its own specific requirements when it comes to "how much" material is removed per pass and which machine is doing the work. Generally speaking, parts are "rough machined" down to within .100" of final dimensions. Then the final clean up (about .010") pass skims off this rough surface to achieve the required size and surface finish. If a tool is dull, then the 125 rms surface finish which is required on all drawings would not be produced. A dull tool produces a smeared or torn surface appearance which is the primary method of monitoring the adequacy of the tooling and the machining process in general. A number of tests on various parts in various heat treated conditions has demonstrated that the most severe operation in terms of surface cold work is generation of the stub Acme threads on the tie rods which serve as a "worst case" bounding condition.

The judgment and experience of the machinist is relied upon to determine how much material can be safely removed per cut or per pass. Written documents could not possibly address all possible eventualities of workpiece size, shape, and material or machine type and capacity or dimensions, tolerances, and surface finish necessary to produce. Vendor inprocess control sheets or travelers are used to control the flow of material in the shop. While in process, machining is seldom, if ever, controlled by fixed documents, the end results are carefully specified on the drawings.

Question 12

Identify the lubricants that would be used on the machined threads during installation. What are the controls of the content of chlorides, sulfides, halogens and other elements that are known to promote stress corrosion cracking in stainless steel and high nickel alloy?

Response 12

The lubricant used for machined threads during installation is thread lubricant D50YP5B. The lubricant is referenced on GE reactor modification drawing parts list.

GE Specification D50YP12 provides the controls of the content of halogens, nitrate, sulfur and other elements in lubricant D50YP5B. The specification defines the requirements for limiting impurities in lubricants that are in crevices exposed to BWR primary reactor coolant at temperatures above 165°F. Impurity limits are as follows:

1. The maximum allowable level of halogens, when both sulfur and nitrates are less than 1 ppm, is 450 ppm.

2. The maximum allowable level of sulfur, when both halogens and nitrates are less than 1 ppm, is 630 ppm.

3. The maximum allowable level of nitrate, when both total halogens and total sulfur are less than 1 ppm, is 820 ppm.

4. Allowable simultaneous levels of halogens, sulfur and nitrates in combination can be determined from the nomograph in Addendum A in the following manner when the values of any two of the impurities are known, or are assumed. Place a straightedge through the two known or assumed values on their scales and read the third value from its scale. The third value must not be exceeded.

5. Allowable combined levels of halogens, sulfur and nitrates can also be determined using the formula below:

$$\frac{\text{ppm Halogens}}{35.453} + \frac{\text{ppm Sulfur}}{48.096} + \frac{\text{ppm Nitrates}}{62.004} < 13.2$$

6. The maximum allowable level of any single low melting point metal is 200 ppm.

7. The maximum allowable level of all low melting point metals in combination is 500 ppm.

Question 13

The staff realizes that the repair assemblies may be inspected by a combination of visual and ultrasonic examinations. However, the staff has some concern regarding the reliability of such inspection to identify the potential degradation in the threaded joints and areas of crevices and stress concentrations, which have limited access for inspection. Please provide a discussion and/or propose an alternative inspection such as disassembling the threaded joints for inspection to ensure that the areas mentioned above in the repair assemblies will be adequately inspected for early detection of potential degradation.

Response 13

The tendency toward stress corrosion cracking is promoted by material type, condition, local water chemistry, applied loads, residual stresses, etc.. In the case of stainless steel threaded fasteners, crevices, surface condition (surface cold work) and sustained tensile stress are of specific concern. For the shroud restraint hardware several factors mitigate the concern for potential stress corrosion cracking.

Material - XM-19

In the middle 1970's in the interest of improving the margin of control rod drive (CRD) performance, GE implemented the use of XM-19 for piston and index tubes in place of Type 304 stainless steel. The logic was that as a low carbon, high chromium, mildly stabilized (Nb,V) austenitic alloy XM-19 would offer a higher margin of resistance to intergranular stress corrosion cracking (IGSCC) in the nitrided condition than Type 304. Nitriding involves heating the material to approximately 1100 degrees F for several hours and results in furnace sensitization of 300 series stainless steels, but has no detectable effect on XM 19. As a side benefit, XM-19 has a significantly higher strength than Type 304 so equivalent components are stressed to a lower fraction of yield stress in service. Since the late 1970's all control rod drives manufactured by GE have contained XM-19 piston and index tubes. This includes all BWR-6s (more than 1500 drives) plus several other BWR-4/5's under construction at the time; as well as, all replacement drives manufactured since. In total there are easily more than 2000 such control rod drives in service.

By the nature of the CRD design there are numerous crevices including threaded joints exposed to the reactor environment. On the average 10 to 20 per cent of the drives at a given plant are refurbished each outage. During this work the drives are disassembled giving ample opportunity for examination and detection of problems. To date no instances of intergranular attack or IGSCC of nitrided XM-19 have been reported.

XM-19 shroud repair hardware material is provided solution annealed at 2000 ± 50 degrees F after completion of final reduction, sizing, and forming operations. All XM-19 material has had sensitization testing performed for each heat and each heat treat lot. The sensitization requirements exceed the requirements ASTM A-262.

Material - X-750

X-750 shroud repair hardware material is provided solution annealed at 1975 ± 25 degrees F after completion of final reduction, sizing, and forming operations. In addition, this material is age hardened at 1300 ± 15 degrees

F. All X-750 has Intergranular attack (IGA) testing performed after annealing for each heat and each heat treat lot.

It should be noted that there are no welds in the shroud restraint design, so there are no weld residual stresses. Also, there is no grinding in the shroud restraint design, so there are no grinding induced residual stresses or cold work. As a consequence, the threaded fasteners in the restraint design experience a relatively low level of sustained tensile stress compared to welded crevice joints.

Finally, machined components that are not solution annealed after machining shall have metallographic and microhardness evaluation on test samples. Samples shall be provided from the same material, same fabrication shop and using the same process variables as the components which are being fabricated for the repair. The purpose of these evaluations is to verify the material's surface condition have very shallow cold work depth. Control of the cold work depth will minimize the materials susceptibility to IGSCC initiation.

Based on the material properties and fabrication processes described above, future disassembly of threaded fasteners, crevices, and stress concentrations areas for the express purpose of inspection is not intended. However, if these areas require disassembly in the future for other reasons, a visual inspection of the threaded, creviced, and stress concentration areas will be performed prior to reassembly. The detailed plans for future inservice inspection of the installed core shroud repair components have not yet been finalized. Quad Cities will submit these plans to the NRC staff at least ninety days prior to the first refueling outage following the outage in which the shroud repair components are installed."

Question 14

Please discuss the reasons that GE selects XM-19 material for the tie rods instead of austenitic 304 or 316 stainless steel (low carbon content). The 304 or 316 stainless steel has extensive service experience in the BWR environment. It should be noted that the acceptable yield strength of XM-19 material is limited to 90 ksi. Since there is limited service experience of XM-19 material in the BWR environment, the staff recommends that an accelerated stress corrosion testing of a mock-up simulating the XM-19 tie rod thread joint in a BWR environment should be performed to ensure there is no development of unexpected degradation.

Response 14

XM-19 has experienced no known failures or other problems in approximately twenty years of BWR service. This is considered to be adequate confirmation that the material is acceptable for use.

XM-19 was extensively studied and tested in the mid-1970s. Results of these tests were published in Document NEDE-21653, of which the NRC received copies in 1977. This document contains all of the applicable test information and will be provided in a separate submittal. XM-19 has experienced no known failures or other problems in approximately twenty years of BWR service. This is considered to be adequate confirmation that the material is acceptable for use.

Operating Experience With XM-19.

In the middle 1970's in the interest of improving the margin of control rod drive(CRD) performance, GE developed and implemented the use of XM-19 for piston and index tubes in place of Type 304 stainless steel. The logic was that as a low carbon, high chromium, mildly stabilized (Nb,V), austenitic alloy, XM-19 would offer a higher margin of resistance to intergranular stress corrosion cracking (IGSCC) in the nitrided condition than Type 304. Nitriding involves heating to ~1100 degrees F for several hours and results in furnace sensitization of 300 series stainless steels. As a side benefit, XM-19 has a significantly higher strength than Type 304 so equivalent components are stressed to a lower fraction of yield stress in service. Since the late 1970's all control rod drives manufactured by GE have contained XM-19 piston and index tubes. This includes all BWR-6s (more than 1500 drives) plus several other BWR-4/5 s under construction at the time as well as all replacement drives manufactured since. In total there are easily more than 2000 such control rod drives in service.

By the nature of the CRD design there are numerous crevices including threaded joints exposed to the reactor environment. On the average 10 to 20 per cent of the drives at a given plant are refurbished each outage. During this work the drives are disassembled giving ample opportunity for examination and detection of problems. To date no instances of intergranular attack or IGSCC of nitrided XM-19 have been reported.

Question 15

Please identify the ASME Code Material Specification Nos. that are specified for the procurement of the XM-19, 316 or 316L austenitic stainless steel and alloy X-750.

Response 15

All of the materials are purchased to American Society for Testing Materials (ASTM) specifications: XM-19 = A182, A240, A336, A412, or A479. 316 or 316L = A182, A240, A336, or A479. X-750 = B637. The materials are identified in the GE fabrication specification.

Question 16

Are Certified Material Test Report (CMTR) and heat treatment records available for all procured materials?

Response 16

All materials procured for these assemblies are purchased with CMTRs. For the most part, and in keeping with the ASTM specifications, heat treatment information on CMTRs is limited to a statement that the material is "in the solution annealed condition", and the holding temperature is given. For the most part the mills do not include furnace charts or other specific details of the process to the suppliers from whom we buy the material. However, we require confirmatory testing, either to ASTM procedures or to GE equivalents of those procedures (such as E50YP20), which assures that the material was adequately and properly heat treated.

CORE PLATE WEDGE ISSUE

1. Introduction

The purpose of this document is to describe the analysis performed to determine if core plate wedges were needed for the Peach Bottom shroud repair. The specific concern to be addressed was that of the horizontal motion of the core plate relative to the shroud during a seismic event. That motion when combined with the shroud horizontal seismic motion at the core plate elevation must meet the deformation limits specified in the design specification.

The method used to evaluate the horizontal motion of the core plate as a whole was to compare the friction force provided by the initial preload clamping force of the core plate studs to the horizontal seismic loads. Conservative localized deflections were assumed to occur between the studs and corresponding core plate holes and due to localized bending of the core plate studs. The total deflection of the core plate resulting from the shroud displacement plus the localized displacement of the core plate relative to the shroud was shown to be within the allowable displacements for all load combinations.

2. Analysis

The configuration with restraint hardware installed but no shroud cracking is non-limiting since the resulting shroud seismic loading is unchanged from the original design basis and the restraint hardware sees very low loads. Therefore, the case of seismic loading with stabilizers installed and a cracked shroud is evaluated.

2.1 Gross Core Plate Deflection

The evaluation determined the net uplift force on the core plate due the combined effects of pressure differences, component weights and vertical seismic accelerations. The values are summarized in Table 1. The Peach Bottom core plate is installed with thirty-four 2½ inch diameter studs with each stud preloaded to approximately 43,500 pounds. Considering relaxation in the studs, the resulting clamping force on the core plate at operating conditions is approximately 1,257,000 pounds. Combining the stud preload with the operational and seismic uplift forces produces the net clamping forces reported in Table 1. Two values of coefficient of friction were considered in the analysis of the horizontal friction force maintained between the core plate and shroud to resist the horizontal seismic loading; 0.2 as specified by the VIP / BWROG and 0.5 which has been widely used in reactor internals design. The more conservative friction values for the 0.2 friction coefficient are given is Table 1. Also shown in Table 1 are the horizontal seismic loads on the core plate which result from the fuel and control rod guide tubes. A comparison of the horizontal seismic loads on the core plate to the friction force available to resist the seismic loading shows the

available friction force to be the significantly larger of the two. Therefore, no gross sliding or relative motion of the core plate relative to the shroud will occur due to the horizontal seismic shear loads.

2.2 Localized Core Plate Deflection

The seismic shear load that is transferred through the core plate into the shroud is not transferred uniformly around the circumference. For an uncracked shroud there is a tendency for more load transfer to occur at 90 degrees from the seismic line of action where the shroud is stiffer. For a cracked shroud with restraints installed, the lower spring provides a hard spot on the shroud at 45 degrees from the seismic line of action and a larger percentage of the seismic load would be transferred there. These non-uniform load paths may cause the friction between the core plate and the shroud to be overcome producing local sliding of the core plate relative to the shroud. The magnitude of the relative sliding will be limited to the sum of the gaps between the stud and the stud hole in the core plate plus the gap between the stud and its hole in the shroud. After these gaps are closed the stud acts as a shear pin with a horizontal stiffness of approximately 174 kip/inch. The total nominal radial gap is 5/16 inch. With stiffness of 174 kip/inch, the relative elastic deformation due to stud bending would be about 0.025 inch if only 17 of the 34 studs are conservatively assumed to resist the 74 kip seismic shear load for the Emergency case. The largest local horizontal motion of the core plate relative to the shroud could therefore be 0.34 inch. From the Peach Bottom seismic results for the shroud repair that appear in GENE-771-60-0994, the gross elastic horizontal seismic motions of the shroud at the core plate elevation are 0.32 inch, 0.67 inch and 0.88 inch for N+U, E and F load combinations respectively. Adding the 0.34 inch local deformation from above to these gross shroud motions results in values of 0.66,1.01, and 1.22 inch for N+U, E and F load combinations which are less than the allowable elastic displacement values from the Design Specification of 0.75, 1.12, and 1.49 inch respectively.

3. Conclusions

3.1 No gross sliding of the core plate as a unit relative to the shroud will occur for any of the load combinations in the Peach Bottom Design Specification for the shroud repair project.

3.2 Local sliding of the core plate relative to the shroud may occur near one or more core plate studs. The magnitude of the local sliding is limited to the gap between the stud and the stud holes in the core plate and shroud plus the elastic deformation of the stud in shear and bending. This resultant local sliding, when added to the gross shroud seismic displacement, is less than the allowable elastic displacements for all load combinations.

3.3 Wedges between the core plate and shroud are not required.

Table 1

Load Condition	Uplift Force on Core Plate (kip)	Net Core Plate Clamping Force (kip)	Available Friction Load (kip)	Horizontal Seismic Load (kip)
Norm + Upset	258	999	200	42
Emergency	260	997	199	74
Faulted	341	916	183	69

GE Nuclear Energy

25A5607	SH NO. 1
REV.4	

REVISION STATUS SHEET

DOC TITLE REACTOR PRESSURE VESSEL

LEGEND OR DESCRIPTION OF GROUPS

	DENOTES CUMULATIVE CHANGES TO REVISION 2

TYPE: STRESS REPORT

FMF: PEACH BOTTOM 2 AND 3

MPL NO: PRODUCT SUMMARY SEC. 7

THIS ITEM IS OR CONTAINS A SAFETY RELATED ITEM YES ☒ NO EQUIP CLASS P

REVISION			C
0	RM-01514 9/24/94		
1	J. L. TROVATO 11/8/94	RJA	
	CN01808 CHK BY: J. L. TROVATO		
2	J. L. TROVATO 11/18/94	RJA	
	CN 01861 CHK BY: J. L. TROVATO		
3	J. L. TROVATO 06/09/95	RJA	
	CN 02616 CHK BY: J. L. TROVATO		
4	J. L. TROVATO JUN 21 1995	RJA	
	CN 02806 CHK BY: J. L. TROVATO		

PRINTS TO

MADE BY	APPROVALS	GENERAL ELECTRIC COMPANY 175 CURTNER AVENUE SAN JOSE CALIFORNIA 95125
J.L.TROVATO 9/22/94	A.S. HERLEKAR 9/24/94	
CHK BY J.L. TROVATO 9/22/94	ISSUED BY R.J. AHMANN 9/24/94	CONT ON SHEET 2

1. SCOPE

1.1 This document is the ASME Code Section III Faragraph N-142 Stress Report for the Reactor Pressure Vessel. This analysis addresses the new loads applied to the vessel as a result of the installation of the shroud stabilizers, which function to replace horizontal welds H1 through H7 and cracking of weld H8 in the core shroud.

2. APPLICABLE DOCUMENTS

2.1 General Electric Documents. The following documents form a part of this stress report to the extent specified herein.

2.1.1 Supporting Documents

a. Code Design Specification 25A5580 Rev. 4

b. Shroud Repair Hardware Design Specification 25A5579 Rev. 3

2.1.2 Supplemental Documents. Documents under the following identities are to be used with this stress report.

None

2.2 Codes and Standards. The following documents of the specified issue form a part of this specification to the extent specified herein.

2.2.1 American Society of Mechanical Engineers (ASME) Boiler and Pressure Vessel Code

a. Section III, 1965 Edition and Addenda through Winter 1965

2.2.2 Other Documents

a. General Electric Drawing 886D449 P2, Sht. 1 Rev. 11

b. General Electric Drawing 886D449 P2, Sht. 7, Rev. 8, "Vessel Loadings"

c. Babcock and Wilcox Report dated May 16, 1973, "Stress Report for Peach Bottom Unit 2 Reactor Vessel" (VPF #1896-146-1)

(1) Report No. 20 "Shell Analysis", Rev. 0

(2) Report No. 11 "Shroud Support System Analysis", Rev. 2

(3) Report No. 10 "Brackets", Rev. 0.

(4) Report No. 8, "Support Skirt Analysis", Rev. 0

d. Babcock and Wilcox Report dated September 5, 1973, "Stress Report for Peach Bottom Unit 3 Reactor Vessel" (#610-0146-51/52)

(1) Report No. 20 "Shell Analysis", Rev. 0

(2) Report No. 11 "Shroud Support System Analysis", Rev. 2

(3) Report No. 10 "Brackets", Rev. 0.

(4) Report No. 8, "Support Skirt Analysis", Rev. 0

e. "Theory of Plates and Shells", by S. Timoshenko, 2nd Edition

f. "Roark's Formulas for Stress and Strain", by W.C. Young, 6th Edition

g. General Electric Drawing No. 112D6490, Rev. 0, "Detail Support, Lower."

h. "Reactor Pressure Vessel Power Rerate Stress Report Reconciliation for Peach Bottom Nuclear Power Plant Units 2 and 3", G.E. Report No. NEDC-32166, Class II, dated January 1998

i. "Fatigue Evaluation of the Peach Bottom II and III Reactor Vessels", G.E. Report No. GE-NE-523-61-0493, dated May 1998.

j. General Electric Drawing No. 729E762, Rev. 0, " Reactor Thermal Cycles."

k. General Electric Drawing No.VPF # 1896-64-7, "Shroud Support."

3. GENERAL DESCRIPTION

3.1 The purpose of the shroud stabilizers is to structurally replace all of the horizontal girth welds in the core shroud and shroud support. These welds were required to both horizontally and vertically support the core top guide, core support plate, and shroud head, and to prevent core bypass flow to the downcomer region. The core top guide and core support plate horizontally support the fuel assemblies and maintain the correct fuel channel spacing to permit control rod insertion.

3.2 The design requirements for the shroud stabilizers were separated into two documents. The first document addressed those requirements that were not under the jurisdiction of the ASME Code (Paragraph 2.1.1.b). The second document addressed those requirements that were under the jurisdiction of the ASME Code (Paragraph 2.1.1.a).

3.3 This Stress Report documents the acceptability of the structural integrity requirements of the Code Design Specification defined in Paragraph 2.1.1.a.

4. ANALYSIS

4.1 The Design Specification (2.1.1.a) defines three new design mechanical loads on the reactor pressure vessel. These loads and their point of application are shown in Figure 1 and Table 1. These loads are separated by a distance of greater than 2.5 $\sqrt{Rt}$ = 70" (2.2.1.a) and therefore, can be treated as separate forces. Each of F1, F2, and F3 are addressed below.

4.2 The force F1 (= 92,900 lbs) is applied to the reactor pressure vessel (RPV) shell 72 inches above the shroud support plate. It is a local force applied in the radial direction by the shroud repair during a maximum credible earthquake (MCE). At this elevation the RPV shell is 6.125 inches thick minimum (2.2.2.c(1)).

4.2.1 Compute stresses induced in RPV due to F_1 = 92.9 kips applied at approximately 72 inches above the support plate during MCE:

Use theory of plate and shells by S. Timoshenko (2.2.2.e. pg. 471)

R_i = 125.5" Inside R of RPV

h = 6.125" Thickness of RPV exclusive of cladding

α = 125.5 + 6.125/2 = 128.563" mean radius

$$\beta = \left(\frac{3(1-\nu^2)}{\alpha^2 h^2}\right)^{1/4}$$

ν = 0.29 Poisson's ratio (2.2.2.c(1))

$$\beta = \left(\frac{3(1-0.29^2)}{128.563^2 \times 6.125^2}\right)^{1/4} = 0.046$$

$M_{Max} = P/4\beta$ and $P = F_1/2l$

where l is contact width of lower contact plate, 5 in.

$$M_{MAX} = \frac{F_1}{(2)(5)(4\beta)} = 50.5\ in-k/in$$

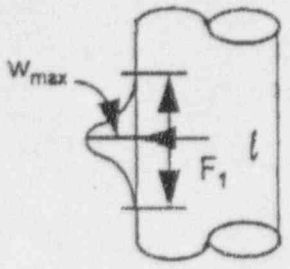

From paragraph 2.2.2.e page 474 deflection under load is

$$W_{MAX} = \frac{P_1\alpha^2\beta}{2Eh} = \frac{9.29 \times 128.563^2 \times 0.046}{2 \times 28.7 \times 10^3 \times 6.125} = 0.02"; \text{ since } E = 28.7 \times 10^3 \text{ ksi (2.2.2.c(1)}$$

$$\sigma_t = 6M_{MAX}/h^2 = 8.08 \text{ ksi}$$

$$\sigma_z = EW_{MAX}/\alpha + 6\nu M_{MAX}/h^2 = 6.81 \text{ ksi}$$

$$\sigma_1 = 8.08 \text{ ksi}$$

$$\sigma_2 = 6.81 \text{ ksi}$$

4.2.2 The maximum value of P_t stress intensity due to this load is negligible and the maximum value of Pb stress intensity due to this load is 8.08 ksi. These stress intensities occur directly under the point of load application.

4.2.3 The existing primary membrane stress intensities in the shell per the original Stress Report (Paragraph 2.2.2.c(1), Page B-9-20) are 26.8 ksi (Pl) and 28.2 ksi (P_t + Pb).

4.2.4 The new value of P_t is same as original value of 26.8 ksi. The new value of Pl + Pb can be conservatively calculated as 28.2 + 8.08 = 36.28 ksi.

4.2.5 The allowable value of primary membrane Pm stress intensity is Sm, which equals 26.7 ksi and the allowable value of primary local (P_l) plus primary bending (P_l + Pb) stress intensity is $3S_m$ = 80.0 ksi for faulted and $2.25\ S_m$ = 60 ksi for emergency conditions. Therefore, both faulted and emergency conditions allowables are met.

4.2.6 Primary stress intensity (Pb) for normal/upset condition F_1 = 33.4 kips = 33.4/92.9 x 8.08 = 2.91 ksi. and primary local stress intensity (P_l) is negligible.

4.2.6.1 The existing P_l = 26.8 ksi. and (P_l + Pb) = 28.2 ksi. The new P_l = 26.8 ksi while new (P_l + Pb) = 28.2 + 2.91 = 31.11 ksi.< 40 ksi (1.5Sm). And since the increase in the stress intensity is very small (2.91 ksi compared to the allowable of 3Sm = 80 ksi for primary plus

secondary stress intensity), the power rerate analysis (2.2.2.h) & fatigue evaluation for revised thermal cycles (2.2.2.i) is unaffected.

4.3 The force F_3 is applied to the reactor pressure vessel (RPV) shell 244 inches above the shroud support plate. It is a local force applied in the radial direction by the shroud repair during a MCE. At this elevation the RPV shell is 6.125 inches thick minimum (Paragraph 2.2.2.c(1).

4.3.1 Stresses in RPV due to F_3 = 31.39 kips applied at approximately 244 inches above the shroud support plate during MCE, can be obtained by scaling from values obtained for F_1 = 92.9 kips with 'ℓ' = 4 inches contact width.

σ_1 = 3.42 ksi

σ_2 = 2.88 ksi

4.3.2 The maximum value of P_l Stress intensity due to this load is negligible and the maximum value of Pb is 3.42 ksi. These stress intensities occur directly under the point of load application.

4.3.3 The existing primary membrane stress intensities in the shell per the original Stress Report (Page B-9-20 of 2.2.2.c(1)) is 26.8 ksi, (P_l) and 28.2 ksi ($P_l + P_b$).

4.3.4 The new value of Pl is conservatively same as existing value of 26.8 ksi. The new value of Pl + Pb can be conservatively calculated as 3.42 + 28.2 = 31.64 ksi.

4.3.5 The faulted allowable value of primary membrane stress intensity is Sm, which equals 26.7 ksi and the allowable value of primary local (P_l) and the primary plus bending ($P_l + P_b$) stress intensity is 3 Sm = 80.0 ksi for faulted and 2.25 S_m = 60 ksi for emergency condition. Therefore, both faulted and emergency conditions allowables are met.

4.3.6 Since the faulted stress intensities (P_l) and ($P_l + P_b$) are below upset condition allowable of 40 ksi., the primary stress intensity for normal/upset condition F_1 = 17,100 lbs is satisfied by inspection as the F_1 is lower than F_3 of MCE condition. And since the increase in the stress intensity is very small [(17.1/31.39) 3.42 =1.87 ksi compared to the allowable of 3Sm = 80 ksi for primary plus secondary stress intensity], the power rerate analysis (2.2.2.h) & fatigue evaluation for revised thermal cycles (2.2.2.i) is unaffected.

4.4 The force F_3 is applied to vertical plate at 4.25 (2.2.2.g) inches from the inside surface of the RPV shell (This results in moment arm of 4.25 + 6.125/2 = 7.3 at RPV shell center line). Since complete load & moment is transfered at shell center line, the analysis in 4.4.1 through 4.4.5 is valid for both weld H8 cracked & uncracked cases. The value of F3 is 372,650 pounds for maximum MCE, and 248,500 pounds for emergency and 172,910 pounds for DBE plus normal pressure & 249,500 pounds for Upset thermal condition. The effects of F_3 on shell are

addressed in 4.4.1 thru 4.4.5 and on baffle plate junction with shell in Section 4.4.6 (H8 uncracked) and Section 4.4.7 (H8 cracked).

4.4.1 Apply F_3 in any condition as vertical load and it will transfer as axial load V = F_3 lbs and moment of 7.31 F_3 k-in. This load V=F_3 kips. and moment 7.31 F_3 k-in. will be assumed to be resisted by the width of RPV shell equal to the width (b = 13.5"), of the horizontal plate of stabilizer lower support (paragraph 2.2.2.g).

4.4.2 Using analysis methods for edge loads for m_o (para. I-233 of 2.2 1.a) and direct membrane stress as P/t, the stresses in shell are as follows:

$$\sigma_t = 6\, m_o / t^2 + P/t;$$

$$\sigma_t = \frac{EW_o}{R_m} + 6\nu \frac{m_o}{t^2}$$

where

m_o = End moment = 7.31 F_3/13.5 k-in/in;

t = Thickness of shell = 6.125";

P = F_3/13.5 kips/in;

E = Young's Modulus = 28.7×10^3 ksi;

R_m = Vessel Mean Radius = 128.5625 in.;

ν = Poisson's ratio = 0.29;

W_o = Deflection at edge (calculated below).

Using para. I-232(2) of 2.2.1.a, the limiting value of $W_o = m_o/2\beta^3 D$, where $D = E\,t^3/12\,(1-\nu^2)$, $\beta = \sqrt[4]{\frac{3(1-\nu^2)}{R_m^2 t^2}}$ and substituting values of D, β in terms of E, t, R_m, the expression for σ_t can be simplified as $\sigma_t = \frac{6m_o}{t^2}\left(\nu + \sqrt{\frac{1-\nu^2}{3}}\right)$. And with $\nu = 0.29$ $\sigma_t = \frac{6m_o}{t^2}(0.84)$.

Further, since t = 6.125", the final σ_t = 0.094 F_3 ksi, σ_t = 0.073 F_3 ksi.

These σ_ℓ, σ_t stresses will be used to calculate the stress intensity by principle stress difference formulas. Since shear stress is zero, the principle stresses are $\sigma_1 = \sigma_\ell$; $\sigma_2 = \sigma_t$. Primary stress intensity is maximum of σ_1, σ_2 or $\sigma_1 - \sigma_2$.

4.4.3 Primary local membrane plus bending ($P_\ell + P_b$) stress intensity for faulted conditions F_3 = 372.65 kips are as follows:

4.4.3.1 $\sigma_\ell = \sigma_1 = 0.094 \times 372.65 = 35.03$ ksi

$\sigma_t = \sigma_2 = 0.073 \times 372.65 = 27.2$ ksi

Thus the maximum primary stress intensity (P_ℓ + Pb) = 35.03 ksi

4.4.3.2 From page B-9-20 of original stress report (2.2.2.c(1)) the existing maximum primary local membrane stress intensity is 26.8 ksi and ($P\ell + P_b$) is 28.2 ksi. And as the major stresses due to F_3 are P_b, i.e; while $P_\ell = 0.007\ F_3 = 2.61$ ksi, P_b is $0.087\ F_3 = 32.42$ ksi out of a total $P\ell + P_b$ of 35.03 ksi. And conservatively the new values will be

$P_\ell = 26.8 + 2.61 = 29.41$ ksi

and $P_\ell + Pb = 28.2 + 35.03 = 63.23$ ksi

However, the maximum P_ℓ , $P_\ell + P_b$ values from page B-9-20 of the existing stress report at location of F_3 (i.e. elem. #20 of Seal Shell model on page B-2-1 of 2.2.2.c(1)), are 17.86 ksi and 19.81 ksi. Thus these values could be used if required.

The allowable P_l and $P_l + P_b$ stress intensity is $1.5S_m$ = 40 ksi in the original stress report. However, this is a faulted event and per 2.2.1.a the allowable for faulted conditions is $3S_m$ = 80 ksi.

4.4.4 Primary stress intensity ($P_l + P_b$) and (P_l) for emergency conditions F_3 = 248,500 lbs are as follows:

4.4.4.1 The primary stress intensity value from 4.4.3.2 for F_3 = 372,650 lbs can be used to get the σ_1 as follows:

$$\sigma_1 = \frac{248500}{372650} \times 35.03 \text{ and } \sigma_1 = \frac{248500}{372650} \times 2.61$$

$= 23.36$ ksi ($P_l + P_b$) $= 1.74$ ksi (P_l)

4.4.4.2 Using same existing maximum primary stress intensity of 4.4.3.2 (for faulted condition) of P_ℓ = 26.8 ksi and $P_\ell + P_b$ =28.2, ksi., the new values are:

$P_l + P_b$ = 28.2 + 28.36 = 51.56 ksi < 60 ksi (2.1.1.a) and P_l = 26.8 + 1.74 = 28.54 ksi < 2.25 S_m = 60 ksi. (2.1.1.a)

4.4.5 Normal/upset conditions evaluations required for primary, primary plus secondary, and peak stress intensities per 2.2.1.a are shown in this section.

4.4.5.1 Primary stress intensity evaluation is required for F_3 = 172,910 pounds which will give ($P_l + P_b$) value of $\frac{172910}{372650} \times 35.03 = 16.25$ *ksi*. and $P_l = \frac{172910}{372650} \times 2.61 = 1.21$ *ksi*

4.4.5.2 The existing primary stress intensity at this location for operating condition is Pl = 17.86 ksi. and $P_l + P_b$ = 19.81 ksi. (page B-9-1 of 2.2.2.c(1)). Thus the new value of $P_l + P_b$ at this location is

$P_l + P_b$ = 19.81 + 16.25 = 36.06 ksi < 1.5 S_m = 40 ksi and P_l = 17.86 + 1.21 = 19.07 ksi < 1.0S_m = 26.7 ksi

4.4.5.3 The primary plus secondary stress intensity for upset condition load F_3 is required for two (2) sets of loading cycles as follows (at RPV shell):

F_3 = 172,910 lbs for 482 cycles normal & excessive heat-up / cooldown transients

and

F_3 = 249,985 lbs for 30 cycles of loss of feedwater pump & HPCI/RCIC injection transients

4.4.5.4 Primary plus secondary stress range for 482 cycles is $S_n = \frac{172,910}{372,650} \times 35.03 = 16.25$ ksi. The existing value of same primary plus secondary stress intensity range is 35.0 ksi (page C-9-21 of 2.2.2.c(1)). Thus the new value of S_n = 35.0 + 16.25 = 51.25 ksi < 3 S_m = 80 ksi.

4.4.5.5 Primary plus secondary stress intensity range for 30 cycles is $S_n = \frac{249,985}{372,650} \times 35.03 = 23.5$ ksi. The existing value of the same primary plus secondary stress intensity range is 35.0 ksi (page C-9-21 of 2.2.2.c(1)). Thus the new value of S_n = 35.0 + 23.5 = 58.5 ksi < 3 S_m = 80 ksi..

4.4.5.6 Fatigue, i.e., peak stress intensity range, evaluation for all 512 (= 482 + 30) cycles per 2.2.2.i is calculated ,using peak stress intensity range of 30 cycles F_3 since it is highest, is as follows:

$S_a = K_e \frac{S_n}{2}$ Since S_n < 3 S_m, K_e = 1.0 for all 512 cycles.

And there is no stress concentration factor per section C-8 of 2.2.2.c(1)

S_a = 27.0 (existing S_a, page C-10-1 of 2.2.2.c (1)) + 23.5/2 = 38.75 ksi.

N_{all} = 8400 (Figure N-415(A) of 2.2.1.a)

Usage Factor = UF = 512/8400 = 0.06 < < 1.0.

Thus the power rerate analysis (2.2.2.h) and fatigue evaluation for the revised thermal cycles (2.2.2.i) is unaffected.

4.4.6 Evaluation of RPV Shell and Baffle Plate Junction(Weld H8 Uncracked)

4.4.6.1 For Faulted Condition F,

Due to the support afforded by jet pump nozzles to the baffle plate, the load F, will be essentially distributed over a rectangular plate between RPV shell and jet pump nozzle hole circle with the width equal to the width of the lower support plate as shown below:.

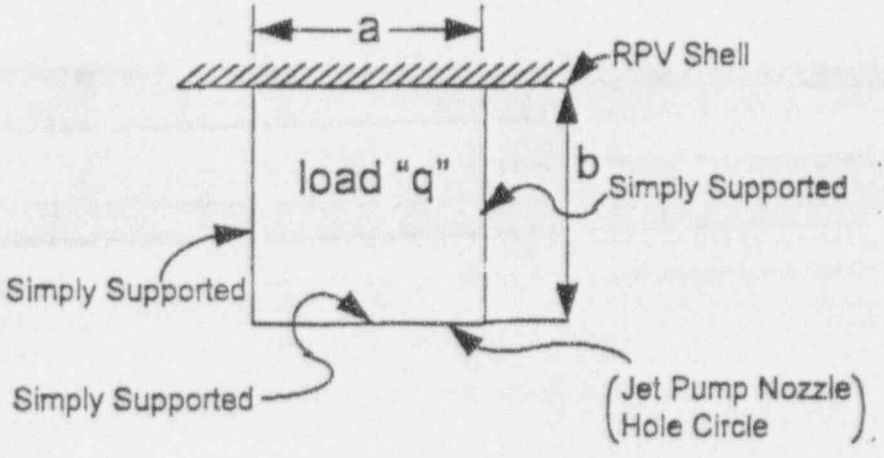

where

a = Width of horizontal lower support plate (2.2.2.g) = 13.5";

b = Distance (radial) between shell inside radius (=125.5") and jet pump nozzle hole circle radius = 226.5/2 = 113.25" (per 2.2.2.k) = 12.25";

q = Distributed load = F3/(13.5 x 12.5) = 372.65/(12.25 x 13.5) = 2.253 ksi;

Using formulas for middle of fixed edge moments (for uniformally loaded plate with one edge fixed, other three edges simple supported) from Timoshenko (2.2.2.e, page 241), the moment

$\overline{My} = d_s q l^2$ (symbols per 2.2.2.3). Further, since b/a = 0.907 d_s = 0.0914 from Table 52 of 2.2.2.e. And since l = 12.25" (smaller of a = 13.5" or b = 12.25"),

$\overline{My}$ = (0.0914) (2.253) $(12.25)^2$

= 30.9 in-kips/in.

Further the bending stress $\sigma_b = 6\ \overline{My}/t^2$ and with t = 2.0625" (thickness of baffle plate), the bending stress value is

σ_b = $30.9 * 6/(2.0625)^2$

= 43.58 ksi

And shear stress $\tau = F_s$/Area = F_s/Perimeter * 't'

τ = 372.65/2 (12.25 + 13.5)(2.0625)

= 3.51 ksi

Principal stress $\sigma_1 = 43.58/2 + [\ (43.58/2)^2 + (3.51)^2\ ]^{1/2} = 43.86$ ksi

σ_y = -0.28 ksi

The maximum stress intensity = $\sigma_1 - \sigma_y$ = 43.86 - (-0.28) = 44.14 ksi

The maximum primary membrane plus bending stress intensity at this location from the existing stress analysis (paragraph 2.2.2.c(2), page B-16-6) is 16.7 ksi. Therefore, the new maximum primary membrane plus bending ($P_l + P_b$) stress intensity is = 16.7 + 44.14 = 61.84 ksi which is less than faulted allowable of 3 Sm = 80 ksi (pages B-17-1, B-17-5 of 2.2.2.c(2)). However, since this junction is also of inconel material and therefore, the 3 Sm of inconel material = 69.9 ksi, being lower than 3 Sm= 80 ksi of carbon steel, the vessel material, will be used as allowable.

Since allowable for (Pl) is same as for (Pl + Pb) and calculated value of Pl is always lower than the calculated value of (Pl + Pb) in all conditions, Pl evaluation is not documented separately for any cases.

4.4.6.2 Primary local membrane plus bending stress intensity (Pl + Pb) for the Emergency condition FS = 248.5 kips is calculated by ratioing down the faulted condition value (Pl + Pb) for loading of 372.65 kips. Thus the new value is (Pl + Pb) = 46.14 ksi which is less than the alowable of 2.25 Sm = 52 ksi for this condition (paragraph 2.1.1.a).

4.4.6.3 Primary stress intensity evalution for upset conditions is required for FS = 172,910 pounds which will give (Pl +Pb) value of 172,910/372,650 x 44.14 = 20.48 ksi.

The existing primary stress intensity for operating conditions is 11.5 ksi (page B-16-8 of 2.2.c(2)). Thus the new value of Pl+Pb at this location is

Pl+Pb = 11.5 + 20.48

= 31.98 ksi < 1.5 Sm = 35 ksi

4.4.6.4 The primary plus secondary stress intensity range for upset condition F3 is required for three (3) sets of loading cycles, (to account modified thermal cycles of 2.2.2.i)as follows (at junction of baffle plate and shell):

F3 = 172,910 lbs for 226 cycles of normal & excessive heatup / cooldown transients

and

F3 = 249,985 lbs for 30 cycles of loss of feedwater pump & HPCI/RCIC transients

and

F3 = 172,910 - 78,200 = 94,710 lbs for 256 cycles of cooldown transient without DBE

4.4.6.5 The primary plus secondary stress intensity range for 226 cycles is Sn = 172,910/372,650 x 44.14 = 20.48 ksi. The existing value of the same primary plus secondary stress intensity range is 51.6 ksi (page B-16-15 of 2.2.2.c(2) range of all cases except case VI See Table 2 for details). Thus the new value of Sn = 51.6 + 20.48 = 72.08 ksi > 3 Sm = 70 ksi. Thus simplified elastic-plastic analysis will be required.

4.4.6.6 The primary plus secondary stress intensity range for 30 cycles is Sn = (249,985 / 372,650) x 44.14 = 29.61 ksi. The existing value of the same primary plus secondary stress intensity range is 72.0 ksi (per B-7-1 of 2.2.2.c(2)only cases III and VI are part of this transient, Table 4 for details). Thus the new value of Sn= 72.0 + 29.61 = 101.61 ksi. which is greater than 3Sm = 70 ksi. Thus simplified elastic-plastic analysis will be required.

4.4.6.7 The primary plus secondary stress intensity range for 256 cycles is Sn = 94,710/372,650 x 44.14 = 11.22 ksi. The existing value of the same primary plus secondary stress intensity range is 31.3 ksi (page B-16-15 of 2.2.2.c(2) maximum of case IV either at bottom or at top). Thus the new value of Sn = 31.3 + 11.22 = 42.52 ksi < 3 Sm = 70 ksi. Thus no simplified elastic-plastic analysis will be required.

4.4.6.8 The peak stress intensity existing range, for 226 cycles is 66.3 ksi (Table 3 stress concentration factor, pg. B-17-2. for details). Thus the new Sp = 66.3 + (20.48)(1.64) = 99.89 ksi where 1.64 is the bending stress concentration factor per page B-17-2 of 2.2.2.c(2).

The fatigue evaluation for 226 cycles F3 is as follows: (Since Sn = 72.08 ksi> 3 Sm = 70 ksi and material parameters of m = 2, n= 0.2 (per pg. B-17-5 of 2.2.2.c(2) Sm < Sn < m 3 S_m)

Ke = 1.0 + [(1-n)/(m-1)n] [S_n/3 S_m - 1] (per 2.2.1.a)

= 1.0 + [0.8/(1x0.2)] [(72.08/70) - 1] = 1.12

Sa = Ke . Sp/2. Since Sn < 3 Sm

Sa = (99.89) (1.12)/2 = 55.94 ksi

Nall = 3,000 (Figure N-415(A) of 2.2.1.a)

Usage Factor = UF1 = 226/3,000 = 0.075

4.4.6.9 The peak stress intensity evaluation for 30 cycles F3 is as follows:(Since Sn = 101.61 ksi > 3 Sm = 70 ksi and material parameters of m = 2, n= 0.2 (per pg. B-17-5 of 2.2.2.c(2) Sm < Sn < m 3 S_m). Thus

Ke = 1.0 + [(1-n)/(m-1)n] [S_n/3 S_m - 1] (per 2.2.1.a)

= 1.0 + [0.8/(1x0.2)] [(101.61/70) - 1] = 2.81

The fatigue evalution for these 30 cycles is as follows: The existing peak stress intensity per page B-17-3 of 2.2.2.c(2) is 146.8 ksi (Table 5 for details).

The extra peak stress intensity for this F3 load is (29.61) (Bending stress concentration factor of 1.64 per page B-17-2 of 2.2.2.c(2)) = 48.56 ksi. The new (total) peak stress intensity Sp = 146.8 + 48.56 = 195.36 ksi. And with Ke = 2.81, the alternating stress Sa = 2.81/2 x 195.36 = 274.48 ksi. The allowable cycles at this Sa level per Figure N-415(A) of 2.2.1.a are 45. Thus usage factor UF2 = 30/45 = 0.67.

4.4.6.10 The peak stress intensity evaluation for 256 cycles F3 is as follows:(Since Sn = 42.52 ksi < 3 Sm = 70 ksi , Ke= 1.0 per 2.2.1.a)

The fatigue evalution for these 256 cycles is as follows: The existing peak stress intensity per page B-17-3 of 2.2.2.c(2) , case IV, is 31.3 ksi.

The extra peak stress intensity for this F3 load is (11.22) (Bending stress concentration factor of 1.64 per page B-17-2 of 2.2.2.c(2)) = 18.4 ksi. The new (total) peak stress intensity Sp = 31.3 + 18.4 = 49.7 ksi. And with Ke = 1.0, the alternating stress Sa = 49.7/2 = 24.85 ksi. The allowable cycles at this Sa level per Figure N-415(A) of 2.2.1.a are 40,000. Thus usage factor UF3 = 256/40,000 = 0.006.

4.4.6.11 The cumulative usage factor (revised) is as follows:

UF = UF1 + UF2 + UF3

The cumulative UF = 0.075 + 0.67 + 0.006 = 0.751 < 1.0 below limits of 2.2.1.a

Thus the power rerate analysis (2.2.2.h) and fatigue evalution for revised thermal cycles (2.2.2.i.) is unaffected.

4.4.7 Evaluation of RPV Shell and Baffle Plate Junction(Weld H8 Cracked)

4.4.7.1 FEM for Weld H8 Cracked Condition

A one quarter finite element model of the baffle plate using computer program ANSYS was analyzed for this condition. The edge of plate at RPV junction was fixed while the junction at shroud was free representing severed H8 weld condition. At lines of symmetry i. e. , 0 degree and 90 degree, proper boundary conditions were used. First unit load case of 449.3 kips vertical load applied as pressure on very small areas (representative case of tie rod load) was analyzed. Second unit load case of uniform pressure of 1,000 psi was also analyzed representing ΔP condition. The results of these unit loading cases are summarized below:

Unit ΔP of 1,000 psi

Pl = 0.5 ksi (0.0005 ksi for ΔP = 1 psi) and Pl + Pb = 442 ksi (0.442 ksi for ΔP = 1 psi)

Pl + Pb + Q = 442 ksi (= 0.442 ksi for ΔP = 1 psi)

Unit tie rod load of 449.3 kips

Pl = 12.6 ksi (0.028 ksi for 1 kip load) and Pl + Pb = 47.5 ksi (0.106 ksi for 1 kip load)

Pl + Pb + Q = 106.8 ksi (0.238 ksi for 1 kip load)

The ΔP values for M. S. LOCA and Normal conditions are = 51 psi & 33.03 psi per 2.1.1.b while, the ΔP value for Upset thermal condition is = 35.68 psi per 2.1.1.b.

4.4.7.2 Evaluation for Faulted Condition

Primary local membrane (Pl) stress intensity for faulted conditions F3 = 372.65 kips is = 0.028 x 372.65 + 0.0005 x 51 = 10.46 ksi which is less than faulted allowable of 3Sm = 70 ksi. for Inconel (baffle plate material) as well as 3Sm = 80 ksi. for carbon steel (RPV shell material). Since allowable for (Pl) is same as for (Pl + Pb) and calculated value of Pl is always lower than the calculated value of (Pl + Pb) in all conditions, Pl evaluation is not documented for remaining cases.

Primary local membrane plus bending (Pl + Pb) stress intensity for faulted conditions F3 = 372.65 kips is = 0.106 x 372.65 + 0.442 x 51 = 62.04 ksi which is less than faulted allowable of 3Sm = 70 ksi. for inconel (baffle plate material) as well as 3Sm = 80 ksi. for carbon steel (RPV shell material).

4.4.7.3 Evaluation for Emergency Condition

Primary local membrane plus bending stress intensity (Pl + Pb) for the Emergency condition load of 248.5 kips is = 0.106 x 248.5 + 0.442 x 51 = 48.88 ksi which is less than 2.25Sm = 52.5 ksi. for inconel (baffle plate material).as well as 2.25Sm = 60 ksi. for carbon steel (RPV shell material).

4.4.7.4 Evaluation for Normal / Upset Conditions

4.4.7.4.1 Evaluation for Primary Stress Intensity

Primary local membrane plus bending stress intensity (Pl + Pb) for the Normal/Upset condition load of 172.91 kips is = 0.106 x 172.91 + 0.442 x 33.03 = 32.93 ksi which is less than 1.5Sm = 35 ksi. for inconel (baffle plate material).as well as 1.5Sm = 40 ksi. for carbon steel (RPV shell material).

4.4.7.4.2 Evaluation for Primary plus Secondary Stress Intensity

The primary plus secondary stress intensity range Sn for upset condition loads of 172.91 kips , 94.71 kips and 249.985 kips is calculated for all loading cycles per 2.2.2.i at junction of baffle plate and RPV shell.

The highest primary plus secondary stress intensity range for 226 cycles of 172.91 kips is Sn = 0.238 x 172.91 + 0.442 x 33.03 = 55.75 ksi, while Sn for 30 cycles of 249.985 kips is = 0.238 x 249.985 + 0.442 x 35.68 = 75.27ksi, and for remaining 256 cycles is = 0.238 x 94.71 + 0.442 x 33.03 =37.14 ksi. All of these Sn values are less than < 3Sm = 70 ksi (conservatively, for baffle plate material), except for 30 cycles of 249.985 kips load. Thus a simplified elastic-plastic analysis will be required for the 30 cycle loading case.

4.4.7.4.3 Evaluation for Fatigue

Since the Sn values in the H8 cracked case are lower than the Sn values for the corresponding cases of 226 cycles, 30 cycles , & 256 cycles under H8 uncracked case, the fatigue, and peak stress intensity range, for all cycles for H8 cracked is enveloped by the similar calculations for H8 uncracked case. Thus the maximum cummulative fatigue usage factor for H8 cracked condition, is conservatively, also equal to 0.751 < 1.0.

4.5 Evaluation for Peach Bottom Unit 2 for F_1, F_2, F_3 and their effects on all code requirements is satisfied as documented in sections 4.1 through 4.4. The original stress report for Peach Bottom Unit 3 (2.2.2.d) states that stress reports 20 (2.2.2.d(1)) and stress report 11 (2.2.2.d(2)) for Unit 3 are exact duplicates of same reports for Unit 2. Hence F_1, F_2, F_3 assessments for Unit 3 is same as shown above for Unit 2 and thus meets all the code (2.2.1.a) requirements. It should be noted that seismic shears and overturning moments for shroud support used in the analysis (page B-11-A of 2.2.2.c(2)) are higher than those required by G.E. Drawing Design (2.2.2.b).

4.6 In accordance with power rerate analysis/reconciliation documentation (2.2.2.h) and fatigue evaluation of Peach Bottom II and III Reactor Vessels for revised thermal cycles (2.2.2.i), there are no changes required to the original stress analysis (2.2.2.c and 2.2.2.d) in the regions affected by loads F_1, F_2, and F_3. Thus power rerate analysis and fatigue evaluation for revised thermal cycles is still valid.

4.7 All of the stress intensities due to the new design mechanical loads F_1, F_2, and F_3 satisfy the allowable stress intensities of the original Code of Construction (Paragraph 2.2.1.a).

4.8 The new seismic loads on the stabilizer bracket location (F_4) is 334,000 lbs for MCE. These when conservatively converted into individual bracket loads (i.e., taken two bracket only in any one directional earthquake) result in individual bracket loads of 167 kips (for MCE). This load is less than the stabilizer bracket seismic loadings of 300 kips (conservatively DBE only) per document 2.2.2.b, Table 9. Thus the effect of F_4 (as a result of shroud stabilizer modification) on RPV is enveloped by the existing stress analysis including fatigue evaluation (2.2.2.c(3)) since page 12 of 2.2.2.c(3) states that it is using seismic loads from 2.2.2.b. Power rerate analysis (2.2.2.h) and fatigue evaluation for revised thermal cycles (2.2.2.i) are not affected since the existing analysis of stabilizer brackets is unchanged and these brackets were not critical components reevaluated in either document 2.2.2.h or 2.2.2.i.

4.9 The new seismic forces and moments on the base of RPV skirt are F5 and M5. The max. of these values (MCE values) are F5 = 284.2 kips and M5 = 6611 kip-ft. These values are less than the seismic values of H_B = 1083 kips and M_B = 40,138 kip-ft (2.2.2.b) which are used in the original skirt stress analysis reports (page B-15-4 of 2.2.2.c(4) and 2.2.2.d(4)) for Peach Bottom Units 2 and 3 respectively. Thus original stress analysis of RPV skirt is still valid. These loads are only primary loads and do not affect fatigue evaluation. The power rerate analysis documentation (2.2.2.h) and fatigue evaluation documentation for revised thermal cycles (2.2.2.i) reevaluates support skirt but since seismic loading used in power rerate is the same as the original loading (2.2.2.b), the power rerate and fatigue evaluation for revised thermal cycles documentation is unaffected by these stabilizer modification forces and moments F5 and M5.

4.10 The new seismic overturning moments and shears at the shroud support location are M_6 = 129.6 k-ft, F_6 = 148.1 kips in MCE. These loads are lower than the seismic moment and shear of 4885 k-ft and 238 kips (conservatively DBE only) per Table 10 of 2.2.2.b. Thus effects of M6/V6 (new) on RPV is enveloped by the existing analysis since page B-11-A of 2.2.2.c(2) states that it is using seismic loads higher than those given in GE drawing (2.2.2.b). The shroud support leg buckling evaluation documented in the original stress report (pages B-18-2 through B-18-9 of 2.2.2.c(2)) is still valid because the seismic overturning moments from the revised analysis are lower than those used in the buckling evaluations. Power rerate analysis (2.2.2.h) and fatigue evaluation for revised thermal cycles (2.2.2.i) are not affected since the existing analysis of shroud support legs is unchanged and these legs were not critical components reevaluated in either document 2.2.2.h or 2.2.2.i.

GE Nuclear Energy

25A5607 SH NO. 17
REV. 4

5.0 Based on the best of my knowledge and belief, it is hereby certified that the analysis documented in this Stress Report satisfies the requirements of ASME Boiler and Pressure Vessel Code Section III, 1965 Edition with Addenda through Winter 1965 and Design Specification listed in Paragraph 2.1.1.a. This certification is provided as required by Paragraph N-142 of said Section III.

Signature: A Sherlekar Date: 6/21/95

License Number: C23562 State: California

Expires on 12/31/1997

REGISTERED PROFESSIONAL ENGINEER
AROON SADASHIV HERLEKAR
C 23562
CIVIL
STATE OF CALIFORNIA

Table 1 - ADDITIONAL DESIGN MECHANICAL LOADS

Force	(Normal/Upset) DBE + Normal Pressure	Emergency	(Faulted) MCE + LOCA	Remarks
F_1	33,400 lbs	92,900 lbs	92,900 lbs	Primary Stress
F_2	17,110 lbs	31,390 lbs	31,390 lbs	Primary Stress
F_3	172,910 lbs	248,500 lbs	372,650 lbs	Primary Stress
	172,910 lbs(w/DBE)	-	-	Pri plus Sec. S.I Range (226 cycles) and fatigue
	94,710 lbs(w/o DBE)	-	-	Pri plus Sec. S.I Range (256 cycles) and fatigue
	249,985 lbs	-	-	Pri plus Sec. S.I Range (30 cycles) and fatigue
F_4	-	-	334,000 lbs	Seismic (Total) Tangential Load @ stabilizer Bracket
F_5	-	-	284,200 lbs	Seismic Shear Only @RPV skirt
M_1	-	-	6,611,000 ft-lbs	Seismic Moment @RPV skirt
M_2	-	-	129,600 ft-lbs	Seismic Moment @Shroud Support
F_6	-	-	143,100 lbs	Seismic Shear @ Shroud Support

1) NOTES

2) F_1, F_2, and F_3 are discrete loads applied over a small area. At any one point in time, F_1, F_2, F_3 are each applied to one location. At any one point in time, F_3 is applied to 4 locations 90° apart for the installation of four shroud stabilizer assemblies. DBE is a Design Basis Earthquake (OBE). MCE is a Maximum Credible Earthquake (SSE). The load F_3 shown is the maximum and applies to one tie rod 180 degrees apart from F_1 & F_2, while remaining tie rods have loads lower than F_3 values shown above.

3) The stress intensities shall meet the stress allowables of the ASME Code, Section III, for the load combinations defined by the Peach Bottom UFSAR. The original Code of Construction did not include Faulted load combinations. Faulted and Emergency load combinations shall meet the stress allowables as defined by the Peach Bottom UFSAR for the reactor pressure vessel.

4) Loads F_1, F_2, F_3 to be used in the evaluations are from document 2.1.1.a. Loads F_4, F_5, M_1, M_2 and F_6 are those for cracked condition as documented in GENE-771-60-0994, Rev. 2.

Table 2

Maximum primary plus secondary stress intensities (P + Q), ksi, for 226 cycles case is range of all cases on page B-16-15 excluding case VI since it is L.O.F.W.P transistion case.

Case	TOP			BOTTOM			2.2.2.c(2)
	H-L	L-R	R-H	H-L	L-R	R-H	Page #
Max. Primary	+6.6	+2.2	+2.4	+1.8	+9.3	+0.3	B-16-15 Case (1)
Min. Primary	-1.2	-8.8	-1.0	-6.0	-2.1	-3.3	B-16-15 Case (2)
Max./Min of cases	+21.0	+9.3	+9.4	+26.2	+0	+11.2	B-16-15
III,IV,V	-6.9	-31.3	-9.2	-8.3	-37.4	-6.3	B-16-15
Total +	+28.5	+11.5	+11.8	+28.0	+9.3	+11.4	Max.
Total -	-8.1	-40.1	-10.2	-14.3	-39.5	-9.9	Min.
Existing Range w/o Case VI	+36.6	+51.6	+22.0	+42.3	+48.8	+21.3	(Max-Min)
Absolute Max. Range	-	+51.6	-	-	-	-	Existing Revised
Contribution From F_s	-	+20.48	-	-	-	-	172.91/372.65* 44.14
Revised Value	-	72.08	-	-	-	-	Max=S_n

Table 3

Maximum primary plus secondary plus peak (P+Q+F) stress intensity in ksi for 226 cycles case is range of all cases on page B-17-3 except case VI since it is L.O.F.W.P. transient case

Case	TOP			BOTTOM	2.2.2.c(2) Page #
	H-L	L-R	R-H		
Case (1) Max. Primary	+11.6	+2.8	+4.1	Since "BOP" envelopes "BOTTOM" only "TOP" is evaluated for peak stress intensities to be consistant with original stress report.	Max. (+), B-17-3
Case (2) Min. Primary	-1.4	-15.6	-1.5		Max (-), B-17-3
Max./min of cases III,IV,V	+21.9	+16.6	+9.4		Max (+), B-17-3
	-6.9	-31.3	-10.1		Min (-), B-17-3
Max. (+)	+33.5	+19.4	+13.5		
Min. (-)	-8.3	-46.9	-11.6		
Range	+41.8	+66.3	+25.1		(Max-Min)
Absolute Max	-	+66.3	-		Existing for 120 cycles
Contribution of F_s	-	53.59	-		1.64*20.48
Sp Revised	-	99.89	-		Existing + Contri. of F_s

GE Nuclear Energy

25A5607 SH NO. 21
REV. 4

Table 4

Primary Plus Secondary Stress Intensity Range (P + Q)

Existing stress report page B-7-1 of 2.2.2.c(2) states that Case VI (which is L.O.F.W.P) is broken into two parts for down ramp i.e. VI iter 32 and VI iter 960 while up ramp is same as Case III. Thus maximum primary plus secondary stress intensities range (ksi) of original analysis for L.O.F.W.P.& HPCI/RCIC transients is as follows.

Case	TOP			BOTTOM			2.2.2.c(2)
	H-L	L-R	R-H	H-L	L-R	R-H	Page #
Case III (up)	-6.9	-2.1	9.0	-8.3	0	8.3	B-16-3
Case VI (max)	-	69.9	-	22.1	11.4	11.2	B-16-3
(min.)	-19.0	-	-50.9	-	-22.2	-33.5	B-16-3
Range (Case VI-Case III)	-12.1	72.0	-59.9	30.4	-22.2	-41.8	-
Absolute Max Range	-	+72.0	-	-	-		Existing Revised
Contribution of F_s	-	29.61	-	-	-	-	(249985/372 650) (44.14)
Revised Value	-	101.61	-	-	-	-	Max S_n

Table 5

Peak Stress Intensity (P + Q + F)

This revised maximum primary plus secondary stress intensity for 30 cycles of this transient is 94.46 ksi which is greater than 3Sm = 80 ksi. Thus simplified elastic-plastic approach will be used for fatigue evaluation. Based on similar statement used for (P + Q) stress intensities, revised (P + Q + F) stress intensities (ksi) are as follows:

Case	TOP			Doc. 2.2.2.c(2) Page #	Remark
	H-L	L-R	R-H		
Case III (up)	-6.9	-2.1	9.0	B-17-3	• Original Report evaluated only "TOP" since it enveloped "BOTTOM" as shown on P + Q evaluation. This is also true for new values as seen on previous page.
Case IV Max.	-	+144.7	+12.2	B-17-3	
Case IV Min.	-68.5	0	-76.2	B-17-3	
Range	-61.6	+146.8	-85.2	Existing Revised	
Absolute Max. Range	-	146.8	-	-	
Contribution of F3	-	48.56	-	(1.64) (29.61)	• Using stress concentration factor for bending = 1.64 page B-17-2 of 2.2.2.c(2)
Revised Sp	-	195.36	-		

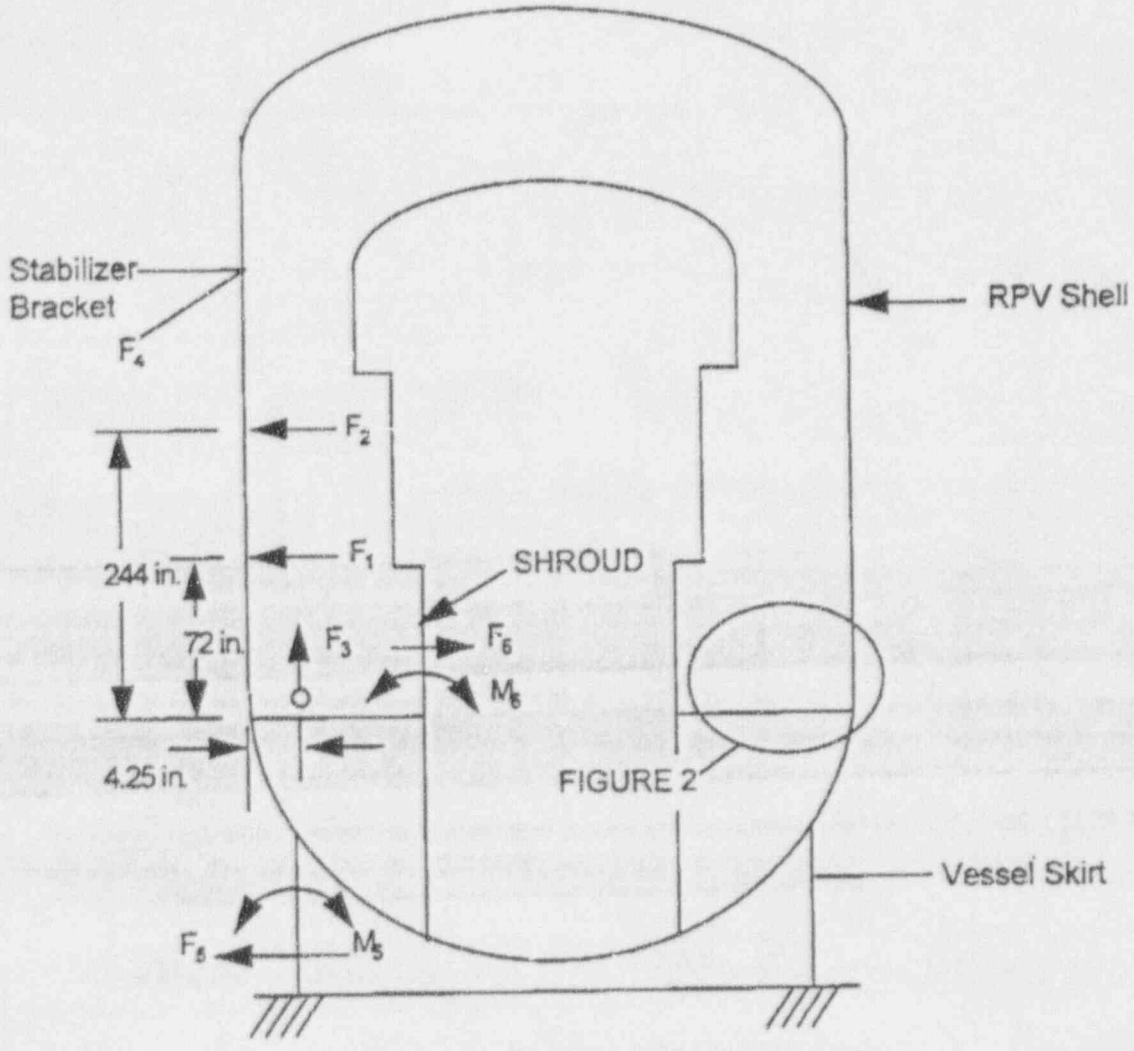

All other dimensions per 2.2.2.a

FIGURE 1. APPLICATION OF DESIGN MECHANICAL LOADS

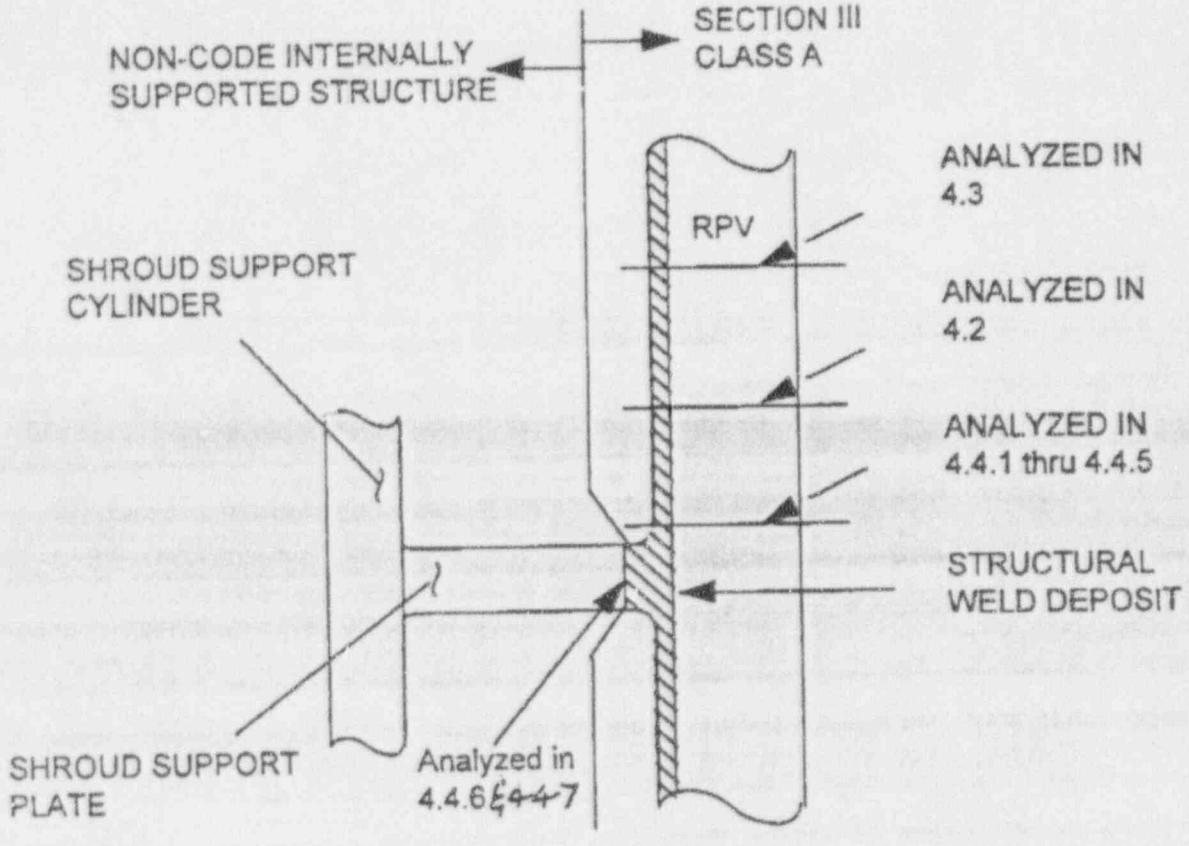

FIGURE 2. BOUNDARY OF ASME CODE JURISDICTION

ATTACHMENT 2

Proprietary Information